TECHNISCHE UNIVERSITÄT WIEN
Vienna University of Technology

Martina Marchetti-Deschmann

DIPLOMARBEIT

Characterization of *"DMG Icon® – Caries infiltrant – proximal"* and its analysis on human teeth by matrix-assisted laser desorption/ionisation time-of-flight mass spectrometry

ausgeführt zum Zwecke der Erlangung des akademischen Grades eines

Diplom-Ingenieurs

unter der Leitung von

Assoc.Prof. Dr. Martina Marchetti-Deschmann

IAC-164
Institut für Chemische Technologien und Analytik
eingereicht an der Technischen Universität Wien
Fakultät für Technische Chemie

von

Eva Kostolányiová, BSc
1635873

Wien, 20. September 2019

Eva Kostolányiová

TECHNISCHE
UNIVERSITÄT
WIEN
Vienna University of Technology

Ich habe zur Kenntnis genommen, dass ich zur Drucklegung meiner Arbeit unter der Bezeichnung

DIPLOMARBEIT

nur mit Bewilligung der Prüfungskommission berechtigt bin.

Ich erkläre weiters an Eides statt, dass ich meine Diplomarbeit nach den anerkannten Grundsätzen für wissenschaftliche Abhandlungen selbständig ausgeführt habe und alle verwendeten Hilfsmittel, insbesondere die zugrunde gelegte Literatur genannt habe.

Weiters erkläre ich, dass ich dieses Diplomarbeitsthema bisher weder im In- noch Ausland (einer Beurteilerin/einem Beurteiler zur Begutachtung) in irgendeiner Form als Prüfungsarbeit vorgelegt habe und dass diese Arbeit mit der vom Begutachter beurteilen Arbeit übereinstimmt.

Wien, 20. September 2019 Eva Kostolányiová

Kurzfassung

Aufgrund von vielversprechenden Ergebnissen, die von der ersten Analyse auf menschlichen Zähnen durch die Forschungsgruppe von Hirano, H. und Mitarbeiter mit matrix-assisted laser desorption/ionisation time-of-flight mass spectrometry (MALDI-TOF-MS) erhalten wurden [1], wurde diese Studie auf eine weitere Anwendung mit ähnlicher Fragestellung fokussiert. Von Interesse ist die Charakterisierung der chemischen Zusammensetzung eines dentalen Füllmaterials, das als synthetische, polymerbasierte Materialprobe beschrieben wird und Detektion des selbigen in Zähnen.

Bei MALDI werden in Matrix eingebettete Analytmoleküle auf einem Probenträger aufgebracht und mit einem Laser beschossen. Die Analyt-Matrix Mischung wird dadurch im Vakuum verdampft und gleichzeitig alle Moleküle ohne Fragmentierung und Zersetzung ionisiert. Die entstandenen Ionen werden durch anlegen einer Hochspannung in Richtung Massenanalysator beschleunigt. Im Flugzeitmassenspektrometer, einem time-of-flight (ToF) Massenanalysator, findet die Bestimmung des Masse-zu-Ladung-Verhältnisses durch Messung der Flugzeit statt. Der Zeitpunkt des Eintreffens der Ionen am Ende der Flugstrecke wird durch einen Detektor nachgewiesen und korreliert mit deren Molekulargewicht [2].

Vorliegende Arbeit gliedert sich in zwei Teile. Der erste Teil enthält die Charakterisierung der chemischen Zusammensetzung des erforschten dentalen Füllmaterials *„DMG Icon® – Caries infiltrant – proximal“* mittels MALDI-TOF-MS. Eine passende Probenvorbereitung und optimale Messbedingungen wurden erarbeitet, die eine Charakterisierung von Icon-Dry und Icon-Infiltrant ermöglichen, zwei Komponenten der kommerziellen Formulierung die am Zahn zu einem Polymer ausgehärtet werden. Des Weiteren wird ein Protokoll zur Probenvorbereitung von Zahnmaterial vorgestellt, wobei Zähne ohne Einbettung als 100 – 700 µm dünne Schnitte durch Schneiden mit einem Diamantsägeblatt vorbereitet wurden. Icon-Infiltrant wurde auf den vorbereiteten menschlichen Zahnschnitten mit 3 verschiedenen Probenvorbereitungsverfahren aufgebracht und per MALDI-TOF-MS gemessen, wobei auch Sublimation als Matrixapplikationsverfahren getestet wurde. Letztendlich wurde die Verteilung von Icon-Infiltrant auf menschlichen Zahnschnitten mittels MALDI Imaging visualisuert.

Abstract

Based on promising results obtained from first analysis on human teeth with matrix-assisted laser desorption/ionisation time-of-flight mass spectrometry imaging (MALDI-TOF-MSI) by Hirano et al. [1], this study was focused on another application of this analytical technique on human teeth samples. The characterization of the chemical composition of a dental filling material described as a synthetic polymer-based material was matter of interest.

For MALDI, the samples are embedded in a crystalline matrix on a target plate and are targeted by laser light. The sample and matrix molecules vaporize in the vacuum while being ionised at the same time without fragmenting. High voltage is then applied to accelerate the charged particles towards the mass analyser. A time-of-flight (ToF) analyser separates ions according to their mass-to-charge ratios and determines the time it takes for each ion to reach a detector [2], which directly correlates to the mass of the particle.

Present thesis is divided into two parts. The first part focusses on the characterization of the chemical composition of the applied dental filling material *„DMG Icon® – Caries infiltrant – proximal“* using MALDI-TOF-MS. Suitable sample preparation procedures were developed and optimal measurement conditions were proposed in order to obtain spectra characterizing Icon-Dry and Icon-Infiltrant, two formulation constitutents of the polymer filling. Sample preparation protocols for the cutting of human teeth into thin sections of 100 to 700 µm thickness without embedding using a diamond blade were established. Subsequently, measurement of Icon-Infiltrant on obtained human teeth sections was performed by applying three different sample preparation protocols. Sublimation is performed as matrix application technique in one of these sample preparation procedures. Eventually, the distribution of Icon-Infiltrant was visualized on human teeth sections by MALDI-TOF-MS Imaging.

Table of Contents

1. Introduction

Over the last two decades, mass spectrometry imaging (MSI) has been increasingly employed to investigate the spatial distribution of a wide variety of molecules in complex biological samples. MSI has already demonstrated its potential for biomedical research and pharmaceutical applications. MSI enables untargeted as well as direct targeted analysis to discover disease-related biomarkers, drug discovery, and disease state evaluation through proteomic and/or metabolic studies. Knowledge of the spatial distribution of molecular species is essential to understand biological processes occuring within tissues [3].

To improve diagnosis and treatment of periodontal disease, matrix-assisted laser desorption/ionisation mass spectrometry imaging (MALDI-MSI) was applied to human teeth for the first time by Hirano, H. and co-workers [1]. Based on obtained results, further application of MALDI-MSI to human teeth is matter of interest.

1.1 Human tooth

The tooth is an ectodermal organ located in mouth whose development is regulated by reciprocal epithelial-mesenchymal interactions [4].

All of the teeth in the mouth together are referred to as the *dentition*. The teeth in the upper jawbones collectively form an arch shape known as the *maxillary arch*, and those in the lower jawbone the *mandibular arch*.

Humans have two sets of teeth in their lifetime. The first set of teeth to be seen in the mouth is the *primary* or *deciduous* dentition and is normally present in a child from the ages of about 2 to 6 years. There are 20 teeth in the entire primary dentition, ten in the upper maxillary arch and ten in the lower mandibular arch. The *permanent* or *succedaneous* teeth replace the exfoliated deciduous teeth and are present in adults. The complete permanent dentition is composed of 32 teeth.

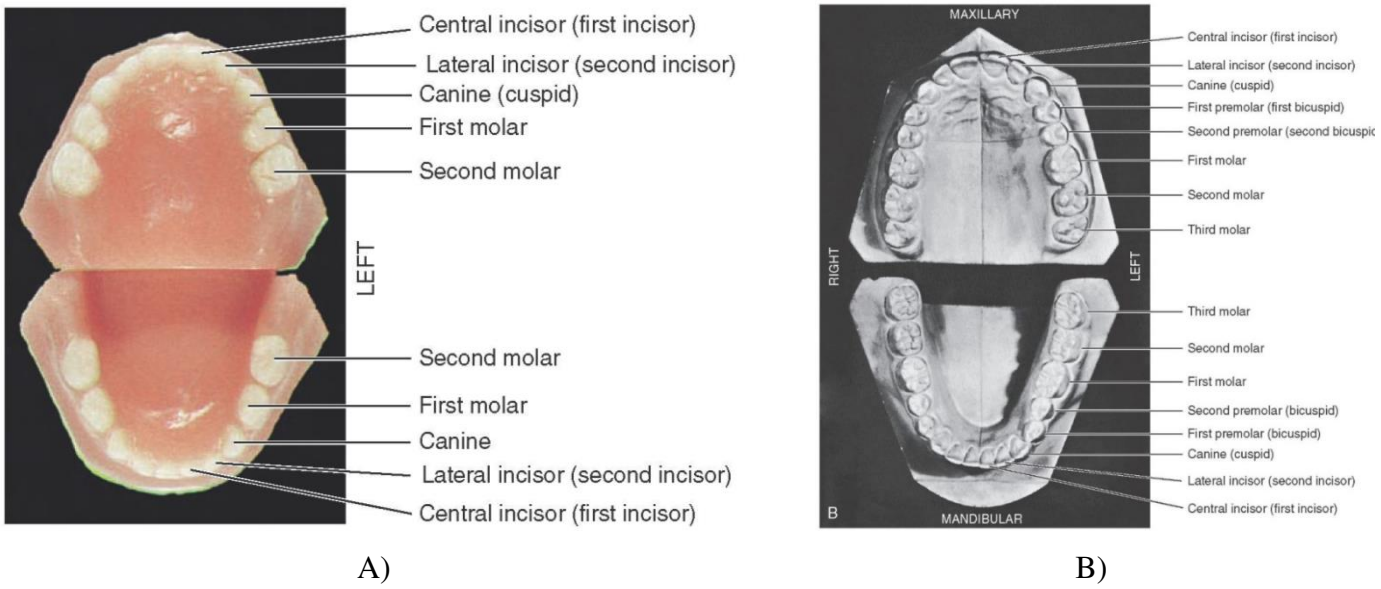

Figure 1 – A) Casts of deciduous dentition. B) Casts of succedaneous dentition. Taken and adapted from https://pocketdentistry.com/1-introduction-to-dental-anatomy/, accessed May 14, 2019.

Each tooth has a **crown** and **root** portion. The anatomic crown is covered by an enamel layer, and the anatomic root is the part of a tooth covered by cementum. The crown and root join at the cementoenamel junction. The root portion of the tooth may be single, with one apex or terminal end, as usually found in anterior teeth and some of the premolars; or multiple, with a bifurcation or trifurcation dividing the root portion into two or more extensions or roots with their apices or terminal ends, as found on all molars and in some premolars. The root portion of the tooth is firmly fixed in the bony process of the jaw.

Teeth consist of four different tissues, **enamel**, **cementum**, **dentin**, and **dental pulp**. The first three are known as *hard tissues*, the last as *soft tissue*. Hard tissues contain considerable mineral content, especially calcium. This high percentage of mineral content is resulting in hardness, durability and damage resistance of human teeth.

Enamel is the white external surface layer of the anatomic crown that covers and protects the dentin. It is highly calcified or mineralized, and is the hardest substance in the body. Its mineral content is 95% calcium hydroxyapatite, the remaining substances include 5% water and enamel matrix.

Cementum is the dull yellow external layer of the tooth root. This part is very thin and is composed of 65% calcium hydroxyapatite, 35% organic matter (collagen fibrils), and 12% water. Cementum

is about as hard as bone but considerably softer than enamel. The main function of cementum is tooth support or tooth anchorage together with the principal fibers and alveolar bone [5].

Cementoenamel junction separates the enamel of the crown from the cementum of the anatomic root. Its clinical location serves as an important anatomical site for measurement of probing pocket depth and clinical attachment level.

Dentin is the hard yellowish tissue underlying the enamel and cementum, and makes up the major bulk of the inner portion of each tooth crown and root. Mature dentin is composed of about 70% calcium hydroxyapatite, 18% organic matter (collagen fibrils), and 12% water. Its main function is to provide support to the enamel. It is also responsible for transmitting impulses from the enamel or root to the dental pulp [6].

Dentinoenamel junction is the inner surface of the enamel cap where enamel joins dentin. Its composition includes type I collagen, phosphorylated and non-phosphorylated proteins [7].

Cementodentinal junction is the inner surface of cementum where cementum joins dentin. This part contains proteoglycans with mucopolysaccharides but containing fewer collagen fibrils than the root dentin and cementum.

Dental pulp is not calcified or mineralized tissue, present in the cavity or space in the center of the crown and root called the pulp cavity. Pulp is soft connective tissue containing a rich supply of blood vessels and nerves. Functions of this portion are as follows:

1) *Formative*: Dentin-producing cells produce dentin throughout the life of a tooth.
2) *Sensory*: Nerve endings relay the sense of pain caused from heat, cold, drilling, sweet foods, decay, trauma, or infection to the brain.
3) *Nutritive*: Blood vessels transport nutrients from the bloodstream to cells of the pulp and the dentin-producing cells.
4) *Defensive* or *protective*: Pulp responds to injury or decay by forming reparative dentin.

Periodontium is defined as the supporting tissues of the teeth in the mouth, including surrounding alveolar bone, the gingiva, the periodontal ligament, and the outer, cementum layer of the tooth roots. The extracellular matrix of these tissues is composed of numbers of the collagen family, proteoglycans and a heterogenous set of glycoproteins.

Alveolar bone is the portion of the upper or lower bones that surrounds the roots of the teeth.

Gingiva is the part of the soft tissue in the mouth that covers the alveolar bone of the jaws. The gingival epithelium plays an important role as a mechanical barrier against bacterial invasion and a part of the innate immune response to infectious inflammation in periodontal disease [8].

Periodontal ligament is a very thin ligament composed of many tissue fibers that attach the outer layer of the tooth root to the thin layer of dense alveolar bone surrounding each tooth [8, 9]. It is the only ligament in the body that connects two distinct hard tissues and its thickness decreases with age. It is functionally important for tooth support, and for allowing the teeth to withstand the forces generated during mastication [9].

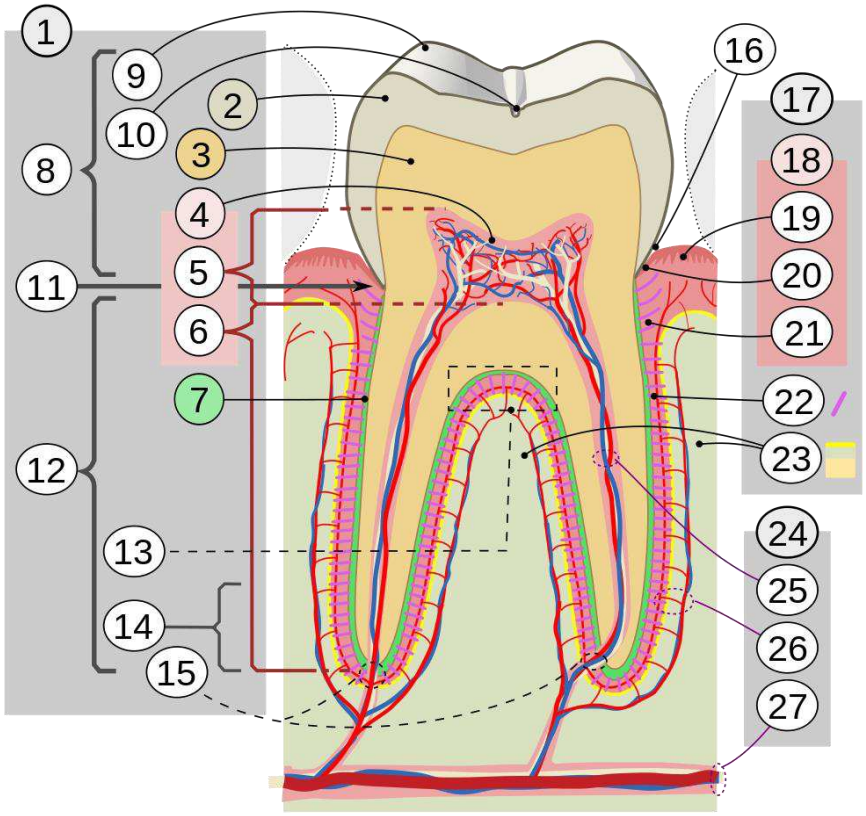

Figure 2 – Cross section of human tooth, multilanguage: 1. Tooth; 2. Enamel; 3. Dentin; 4. Dental Pulp; 5. Cameral Pulp; 6. Root Pulp; 7. Cementum; 8. Crown; 9. Cusp; 10. Sulcus; 11. Neck; 12. Root; 13. Furcation; 14. Root apex; 15. Apical Foramen; 16. Gingival Sulcus; 17. Periodontium; 18. Gingiva: 19. Free or Interdental, 20. Marginal, 21. Alveolar; 22. Periodontal Ligament; 23. Alveolar Bone; 24. Vessels and Nerves: 25. Dental, 26. Periodontal, 27. Alveolar through channel. Nogué, J. M. i. *Cross sections of human tooth.* 2013, https://commons.wikimedia.org/wiki/File:Cross_sections_of_teeth_intl.svg#/media/File:Cross_sections_of_teeth_intl.svg, accessed March 3, 2019.

1.2 Mass spectrometry

Mass spectrometry is an instrumental method for identifying the chemical constitution of a substance (inorganic or organic compound) by means of the separation of gaseous ions according to their differing mass and charge [10]. The information delivered by mass alone can be sufficient for the identification of elements and the determination of the molecular formula of an analyte. In addition, it allows the examination of fragmentation pathways of selected ions and study of ion-neutral reactions and more [11].

Elements which a mass spectrometer always contains can be seen in Figure 3.

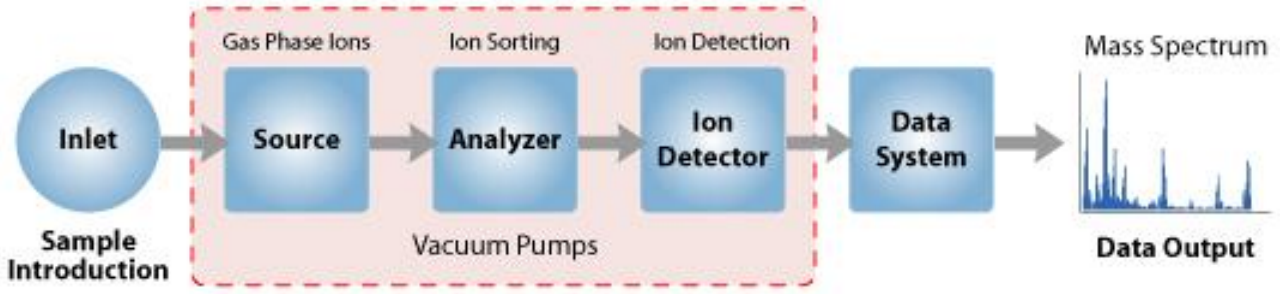

Figure 3 – Components of a mass spectrometer. This image was taken and adapted from the internet [12].

Sample inlet for the introduction of a compound to be analysed is direcetly followed by the ionisation source. In this step, atoms or molecules are ionised in an ionisation chamber and gas phase ions are generated. Respectively, neutral species either loose or gain charges to convert in to ionic forms [13]. The choice of ionisation technique is also influenced by volatility of sample and most important ionisation techniques are listed here:

- Electron Ionisation (EI)
- Chemical Ionisation (CI)
- Field Ionisation (FI)
- Laser Desorption (LD)
- Thermospray Ionisation (TI)
- Plasma Desorption (PD)
- Atmospheric Pressure Chemical Ionisation (APCI)

- Matrix Assisted Laser Desorption Ionisation (MALDI)
- Secondary Ion Mass Spectrometry (SIMS) [14].

Acceleration of ions towards one or several mass analysers with subsequent separation occurs. All mass analysers use dynamic or static magnetic and electric fields that can be alone or combined. Combination of different analysers increases the versatility and allows performing mutiple experiments. Types of analysers with different principles of separation used in MS are listed here:

- Quadrupole (Q) – Mass-to-charge ratio (Trajectory Stability)
- Ion Trap (IT) – Mass-to-charge ratio (Resonance Frequency)
- Time of Flight (TOF) – Velocity (Flight Time)
- Fourier Transform Ion Cyclotron Resonance (FTICR) – Mass-to-charge ratio (Resonance Frequency)
- Fourier Transform Orbitrap (FT-OT) – Mass-to-charge ratio (Resonance Frequency)

The beam of ions reaches the detector responsible for detecting the ions emerging from the last analyser. Afterwards, investigation of the data carried out by computer can begin. A mass spectrum of the molecule is produced and it provides this result as a plot of ion abundance versus mass-to-charge ratio (*m/z*). Software allows an assignment of obtained mass spectra to certain compounds by their comparison to mass spectra present in database.
Matrix-assisted laser desorption/ionisation time-of-flight mass spectrometry (MALDI-TOF-MS) is applied in this study and therefore its principles are discussed more intensively in following chapter 1.2.1.

1.2.1 Matrix-assisted laser desorption/ionisation time-of-flight mass spectrometry

In MALDI-TOF-MS, a MALDI ion source is combined with a TOF analyser. MALDI is a soft ionisation, which provides production of intact gas-phase ions from a broad range of large, non-volatile and thermally labile compounds such as proteins, lipids, oligonucleotides, synthetic polymers and large inorganic compounds [15]. It should be emphasized that MALDI, along with electrospray ionisation, are considered to be the most important ionisation methods for

biomolecules [16, 17]. In TOF analyser, ions are accelerated using an electrostatic field and reach a kinetic energy of several kilo-electronvolts. After leaving the source, ions pass through a field-free time-of-flight tube and are sorted according to their *m/z*. Separation is possible due to the different velocity of ions that have the same kinetic energy but different *m/z* ratios. Because ions with different *m/z* values, but with the same kinetic energy, reach different velocities, separation depending on *m/z* values is possible. Knowing the acceleration voltage and the flight length of ions in a field-free TOF tube enables determination of the *m/z* values of the ions.

After passing the acceleration voltage U the kinetic energy E_{KIN} of ions is defined as:

$$E_{KIN} = \frac{1}{2}mv^2 = zeU \tag{1.1}$$

Where: m = mass of an ion

v = speed of the ion after the acceleration distance

z = charge state

e = elementary charge

The speed v results from the time-of-flight t that an ion needs to cross the field-free time-of-flight tube length L:

$$v = \frac{L}{t} \tag{1.2}$$

Insertion of (1.1) in (1.2) results in:

$$E_{KIN} = \frac{1}{2}m\,\frac{L^2}{t^2} = zeU \tag{1.3}$$

Recalculation to *m/z* results in:

$$\frac{m}{z} = \frac{2eUt^2}{L^2} \tag{1.4}$$

These equations show that the ratio of molecular mass and charge is propotional to the square of the time-of-flight using a TOF mass spectrometer [14].

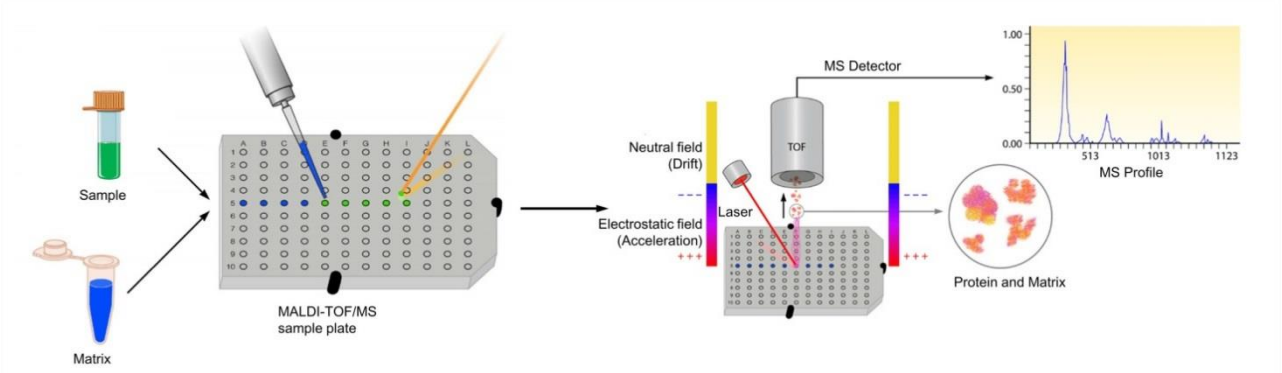

Figure 4 – Schematic representation of MALDI-TOF-MS. This image was taken and adapted from the internet [18].

MALDI is achieved in two steps. Firstly, the compound to be analysed is dissolved in a solvent containing small organic molecules, called the *matrix*. Several methods have been used for matrix application: 1) Manually spraying the matrix solution with a nebulizer sprayer, 2) automatically depositing an array of small droplets of matrix solution with robotic devices, and 3) sublimating the matrices under reduced pressure and elevated temperature [19].

In the present thesis, sublimation was performed as matrix application technique in one of three sample preparation procedures applied on human teeth sections (chapter 2.2.7.2). Home-built sublimation apparatus was used to sublime matrix. This allows optimized matrix application exhibiting small crystal sizes and high reproducibility of sublimation. This home-built sublimation apparatus was firstly introduced by Matthias Holzlechner as a part of his dissertation thesis at the Institute of Chemical technologies and Analytics, TU Wien [20].

When preparation of mixture is accomplished, process of drying can follow. Drying of this mixture before analysis is resulting in removal of any liquid solvent used in preparation of the solution and outcome of this process is an analyte co-crystallized with matrix [15]. Incorporation of the analyte into the matrix crystal lattice is required for MALDI process [14]. MALDI-MS analyses require highest purity matrices and reagents, as organic or trace metal contamination cause adverse effects during crystallization, ionisation and measurement [21]. Matrix compounds must meet a number of requirements simultaneously. They must have a strong absorption at the laser wavelength, vacuum stability, ability to promote analyte ionisation, solubility in solvents compatible with analyte and lack of chemical activity. List of common MALDI matrices is shown in Table 1:

Table 1 – List of common MALDI matrices and their selection according to the class of analyte.

Matrix	Analyte
α-Cyano-4-hydroxycinnamic acid (α-CHCA) 3,5-Dimethoxy-4-hydroxycinnamic acid (SA)	Peptides/proteins
Trihydroxyacetophenone (THAP) 3-Hydroxypicolinic acid (HPA)	Oligonucleotides
2,5-Dihydroxybenzoic acid (DHB) α-Cyano-4-hydroxycinnamic acid (CHCA) Trihydroxyacetophenone (THAP)	Carbohydrates
Dithranol (DIT) *Trans*-2-[3-(4-*tert*-Butylphenyl)-2-methyl-2-propenylidene]malononitrile (DCTB)	Synthetic polymers
2,5-Dihydroxybenzoic acid (DHB)	Synthetic polymers Organic molecules
Dithranol (DIT)	Lipids

Secondly, in the ion source of the mass spectrometer the crystalline surface of a prepared sample is exposed to a laser impulse of short wavelength for a few nanoseconds in vacuum. The irradiated spot is rapidly heated, which causes localized sublimation of the matrix crystals. Expansion of the matrix molecules into the gas phase follows, carrying analyte molecules as well [15].

The required energy to form ions comes from UV-radiation by resonant excitation of matrix molecules such as the π-electron system of aromatic compounds. By using excessive radiation the sample is destroyed. Numerous experiments suggest that the matrix has an important role in the ionisation process of sample molecules. Photoionised, radical matrix molecules result in a high yield of electrically charged sample molecules by proton transfer [14].

It is important to point out that one of the factors that influences MALDI-TOF-MS analyses both in terms of sensitivity and resolution is sample preparation. Thus, the major challenge for studies is to identify its optimal procedure. This is of particular importance in the case of biological specimen contained in physiologic fluids where very often low amounts of an investigated material are available for experiments, and additionally, it is complex and not purified. Since the introduction of MALDI, different procedures in the subsequent stages of sample preparation were tested.

This technique can be used in profiling (MALDI-TOF-MS) and imaging mode (MALDI-TOF-MSI) to detect biomolecules directly from tissue sections. MALDI-TOF-MSI combines the sensitivity and selectivity of mass spectrometry with the spatial analysis provided by traditional histology, offering unbiased visualization of the spatial arrangement of biomolecules in tissue. During the experiment, specific regions of the tissues are irradiated by a laser in an array of discrete points and mass spectra are generated for each x,y coordinate. Ion intensities are then plotted on a coordinate system matching the relative location of each spectrum that was acquired on the tissue surface, creating images of the ion. For reference, MSI images may also be compared to a histological stained micrograph of the tissue to determine molecular patterns that correlate to specific anatomic features [22].

1.3 First application of MALDI-TOF-MSI to human teeth

To explain valuable outcome of applied MALDI-TOF-MSI to human teeth for the first time, conventional techniques during diagnostic procedure and investigated oral diseases will be introduced at first.

Numerous methods or techniques can be used for diagnosis of tooth related illnesses. X-rays (Dental radiography), CAT (Computerized axial tomography) and i-CAT® 3D (3D X-ray technology) scan imaging are often included during diagnostic procedure [23, 24]. Dental radiography is routinely performed in dental clinics and allows dentists to find problems that might otherwise remain undetected, such as bone loss, decay between teeth and problems inside a tooth or below the gum line – the line separating the gum from the exposed part of the tooth [25]. CAT scans are primarily used to enable faster and more accurate fitting of dental implants, but can also be used to assess teeth and risks associated with dental surgery [26].

Dental caries (tooth decay) and periodontal disease (gum disease) are the most common oral health diseases [27]. Both of these diseases are initiated by specific bacteria, and the diseases are modified by host and environmental factors. *Streptococcus mutans*, *Streptococcus sobrinus* and *Lactobacilli* are the main cause of tooth decay [28]. The bacteria associated with periodontal disease are predominantly gram-negative anaerobic bacteria and may include *Aggregatibacter actinomycetemcomitans*, *Porphyromonas gingivalis* and *Prevotella intermedia* [29]. Dental caries results in destruction of tooth structure by acid-forming bacteria in dental plaque in the presence of sugar [30]. Periodontal disease is an inflammation of periodontal tissue and is classified by grade

into gingivitis and periodontitis. Periodontal tissue includes four defined structures: gingiva, cementum, alveolar bone and the periodontal ligament (see Figure 2: mentioned structures labeled with numbers 18, 7, 23 and 22). Gingivitis is inflammation only in the gingiva and is treatable. The earliest indication of gingivitis on a microscopic level involves an increase in inflammatory cells and breakdown of the connective tissue (collagen) in the gingiva. This leads to an increase in tissue fluids (edema, that is, swelling), proliferation of small blood vessels (redness), and some loss of the integrity of the epithelium (ulceration) [31]. In periodontitis, the gingiva, the periodontal ligament, bone and cementum are at risk for breakdown during inflammation with resultant loss of bone height and periodontal ligament. This occurs when inflammatory breakdown extends from the gingiva to the periodontal ligament and bone and when the junctional epithelium (which normally attaches to tooth at the cementoenamel junction) migrates apically onto the root because the connective tissue attachment has broken down [31].

In the past few decades, progress has been made in dental imaging techniques which allowed fascinating new insights into three-dimensional anatomy of tooth and the mouth structures which surround and support the tooth [32]. To improve diagnosis and treatment of periodontal disease, MALDI-TOF-MSI was applied to human teeth for the first time by Hirano, H. and co-workers. By comparing anatomical structure of tooth affected with periodontal disease with normal one, they analysed traces of the disease on tooth. Signals specific to the anatomical structures of tooh i.e., enamel, dentin, dental pulp and periodontal ligament were obtained in mass spectra from healthy tooth. Aferwards, ion images of a normal tooth were reconstructed.

Next, analysis was performed upon tooth with periodontal disease. Ion images, reconstructed using signals from the tooth of periodontal disease, revealed loss of periodontal ligament – one of the features of periodontal disease, while the other dental structures showed no damage. Moreover, ion image depicted an accumulation of signal at *m/z* 496.3 at root surface. Previous studies about inflammation revealed that the signal at *m/z* 496.3 reflects lyso-phosphatidylcholine (LPC), which plays a key role in inflammation. Such an accumulation that cannot be examined only from mass spectrum was revealed by utilization of MSI. Averaged mass spectra including ion images obtained from a normal tooth can be seen in Figures 5 – 7. Averaged mass spectra including ion images obtained from the tooth of a patient with periodontal disease can be seen in Figures 8 – 10.

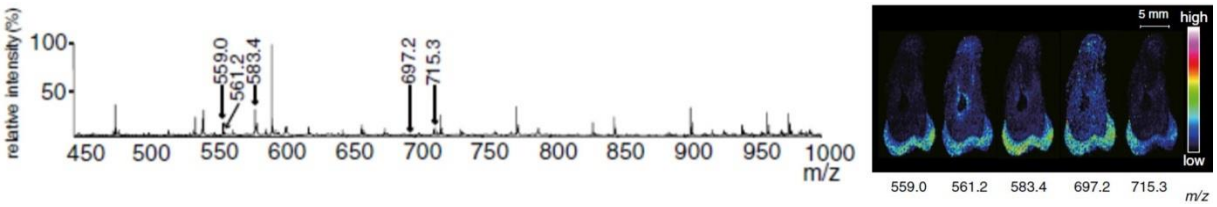

Figure 5 – Left - Averaged mass spectrum of enamel obtained from a normal tooth. Right - Ion image reconstructed from the MSI data of a normal tooth. Signals presumed to be characteristic of enamel, were visualised using a pseudo color scale. Retrieved from Hirano, H. et al., 2013, p. 1358-1359 [1].

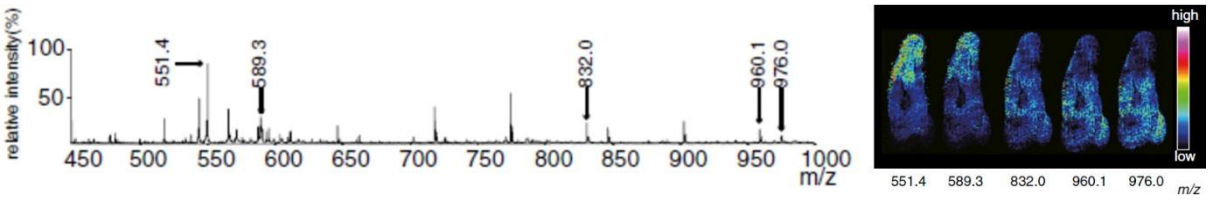

Figure 6 – Left - Averaged mass spectrum of dentin obtained from a normal tooth. Right - Ion image reconstructed from the MSI data of a normal tooth. Signals presumed to be characteristic of dentin, were visualised using a pseudo color scale. Retrieved from Hirano, H. et al., 2013, p. 1358-1359 [1].

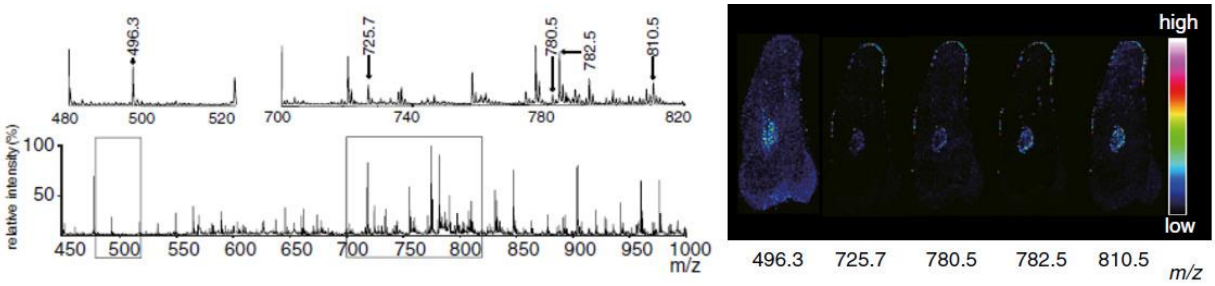

Figure 7 – Left - Averaged mass spectrum of dental pulp obtained from a normal tooth. Right - Ion image reconstructed from the MSI data of a normal tooth. Signals presumed to be characteristic of dental pulp, were visualised using a pseudo color scale. Retrieved from Hirano, H. et al., 2013, p. 1358-1359 [1].

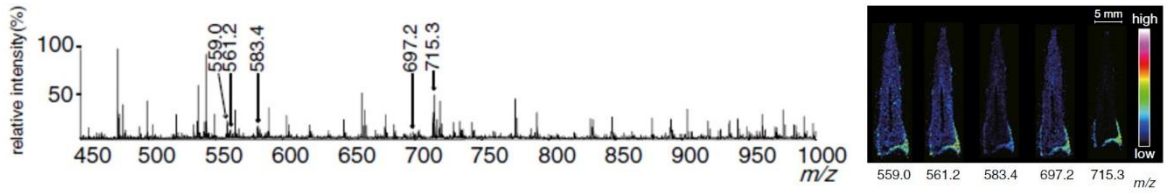

Figure 8 – Left - Averaged mass spectrum of enamel obtained from the tooth of a patient with periodontal disease. Right - Ion image reconstructed from the MSI data. Signals presumed to be characteristic of enamel, were visualised using a pseudo color scale. Retrieved from Hirano, H. et al., 2013, p. 1360-1361 [1].

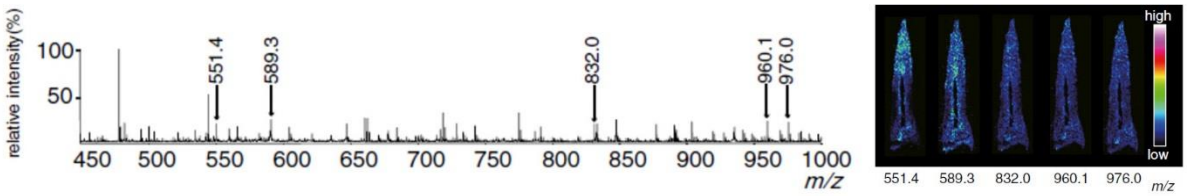

Figure 9 – Left - Averaged mass spectrum of dentin obtained from the tooth of a patient with periodontal disease. Right - Ion image reconstructed from the MSI data. Signals presumed to be characteristic of dentin, were visualised using a pseudo color scale. Retrieved from Hirano, H. et al., 2013, p. 1360-1361 [1].

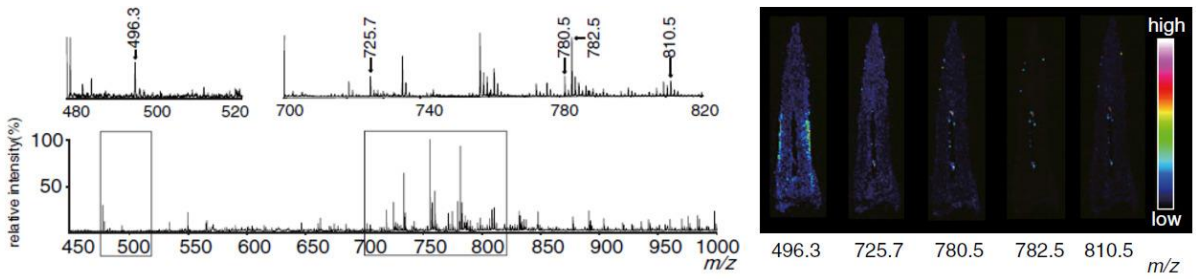

Figure 10 – Left - Averaged mass spectrum of dental pulp obtained from the tooth of a patient with periodontal disease. Right - Ion image reconstructed from the MSI data. Signals presumed to be characteristic of dental pulp, were visualised using a pseudo color scale. Retrieved from Hirano, H. et al., 2013, p. 1360-1361 [1].

To analyse the localization of the signal at *m/z* 496.3 quantitatively, the signal in the teeth of patients with periodontal disease and healthy subjects were compared using a statistical test. The signal intensity exhibited an exponential decrease according to the distance from the root surface corresponding to 1.35 mm. Infiltration of the signal is statistically significant and suggests that

influence of periodontal disease is not only inflammation in periodontal tissue but also infiltration of LPC to root surface. This leads to suggestion that anti-inflammatory treatment is required in addition to the conventional treatment such as removal of contaminants. At last, it may be concluded that application of this modality in patiens with periodontal disease revealed, for the first time, the loss of periodontal ligament and accumulation of LPC as traces of the disease. [1].

1.4 DMG Icon® – Caries infiltrant – proximal

In this chapter, short introduction to white spot lesions and "*DMG Icon® – Caries infiltrant – proximal"* as alternative for micro-invasive treatment of early, non-cavitated caries in the proximal area will be elucidated.

White spot lesions are defined as enamel surface and subsurface demineralisation without cavitation. These manifestations represent the first clinical observation of the progression of dental caries with the possibility of being reversed. These lesions are characterised by a white chalky, opaque appearance [33].

Several approaches have been proposed for the management of non-cavitated carious lesions: Remineralisation of the lesion with topical fluoride application using fluoride rinses or fluoride varnishes with tri-calcium phosphate [34]; casein phosphopeptide-amorphous calcium phosphate pastes (CPP-ACP) [35] fluoride associated to CPP-ACP (Tooth Mousse- Mi Paste plus, GC, Tokyo, Japan); pastes made of hydroxyapatite, fluorine and xylitol (Remin-Pro, Voco Gmbh, Cuxhaven, Germany) [36]; microabrasion with 18% hydrochloric acid and pumice. However, these treatment options have limitations as they do not give immediate result, require patient compliance and stain from external sources may get incorporated into lesions during remineralisation [37].

Infiltrating resinous polymers are considered as an 'ultra conservative' or 'non-invasive' approach. A dedicated resin with low viscosity and high penetration coefficient was developed and is commercially available since March 2009 [38]. Achievable penetration depths and capacity of arresting the progression of caries using different low-viscous materials, various pretreatments and suitable application times have been reported by several studies [39-41].

Icon resin consists of a kit containing three syringes: Icon-Etch - Hydrochloric acid, Pyrogenic Silicon acid and Surfactant-based; Icon-Dry – 99% Ethanol and Icon-Infiltrant – the infiltrating Methacrylate-based resin [37]. After the surface area of the lesion is eroded with 15% HCl gel,

Icon-Dry is applied onto the lesion site. [42]. Chemical structrures of Icon-Infiltrant contitutents can be seen in Figure 11.

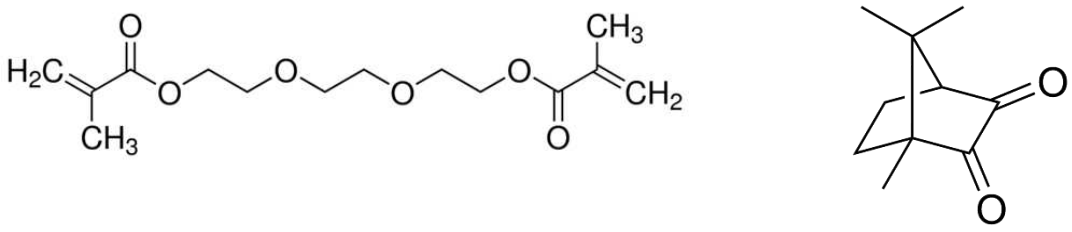

Figure 11 – Left - Triethylene glycol dimethacrylate (TEDMA); Right - Camphoro Quinone. Images were taken and adapted from the website of Sigma-Aldrich company [43, 44].

2. Materials and Methods

This chapter begins with an overview of chemicals used in the present study including their purity and purchasing company (Table 2). Materials and instruments applied in sample preparation procedures and measurements can be found in Table 3. Structures of relevant matrices for this study and image of modified Waters target plate with 6 cavities of different depths used in measurement with human teeth sections can be seen in Figure 12 and Figure 13.

Table 2 – Left column - chemicals; middle column - purity; right column - purchasing company.

Chemical	Purity	Purchasing company
α-Cyano-4-Hydroxycinnamic acid (α-CHCA)	≥ 98%	SIGMA-ALDRICH, St. Louis, USA
2-Propanol	≥ 99.99%	MERCK KGaA, Darmstadt, Germany
2',4',6'-Trihydroxyacetophenone monohydrate (THAP)	98%	SIGMA-ALDRICH, St. Louis, USA

Chemical	Purity	Purchasing company
2,5-Dihydroxybenzoic acid (2,5-DHB)	98%	MERCK KGaA, Darmstadt, Germany
Acetone	≥ 99.5%	SIGMA-ALDRICH, St. Louis, USA
Acetonitrile	≥ 99.99%	SERVA Electrophoresis GmbH, Heidelberg, Germany
Dithranol	≥ 98.0%	SIGMA-ALDRICH, St. Louis, USA
Methanol (MeOH)	≥ 99.99%	MERCK KGaA, Darmstadt, Germany
Peptide calibration Mix 4 (Proteomix) 500-3500 Da	-	LaserBio Labs, Sophia - Antipolis Cedex, France
Silver trifluoroacetate (AgTFA)	≥ 99.99%	SIGMA-ALDRICH, St. Louis, USA
Sodium trifluoroacetate (NaTFA)	98%	SIGMA-ALDRICH, St. Louis, USA
Sodium chloride (NaCl)	≥ 99.5%	MERCK KGaA, Darmstadt, Germany
Tetrahydrofuran (THF)	≥ 99.5%	MERCK KGaA, Darmstadt, Germany
Toluol	≥ 99.99%	MERCK KGaA, Darmstadt, Germany

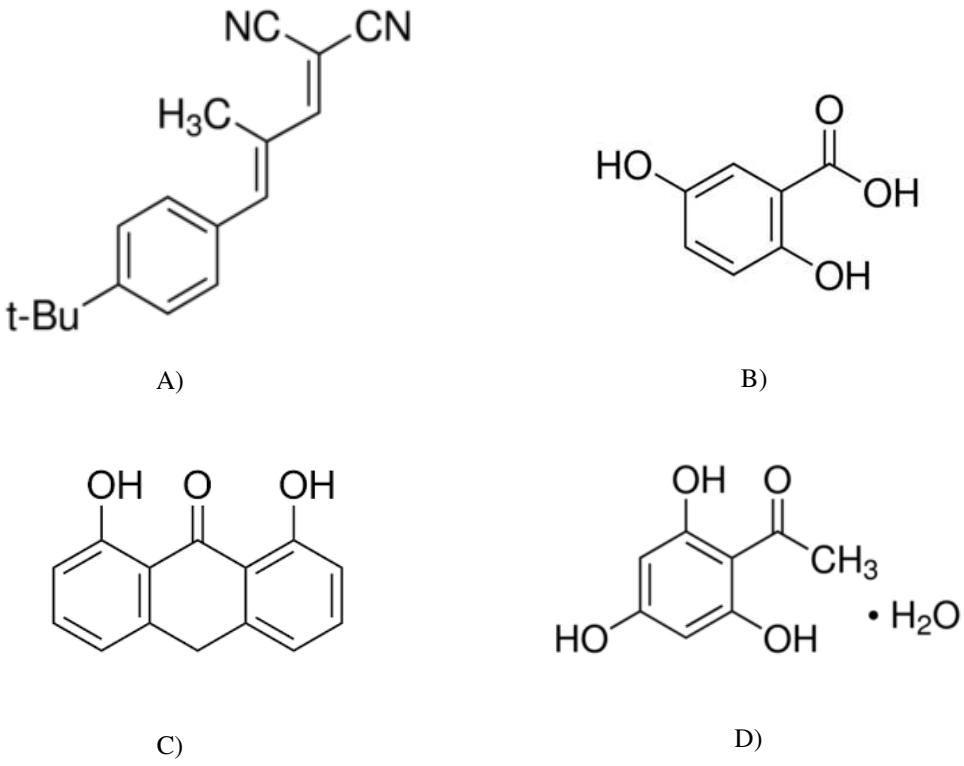

Figure 12 – Chemical structures of matrices applied in this study: A) DCTB B) 2,5-DHB C) Dithranol D) THAP. Images were taken and adapted from the website of Sigma-Aldrich company [45-48].

Table 3 – List of materials and instruments used in sample preparation and measurement procedures of this study.

Material / Instrument	**Purchasing company**
AGAR Gold-Sputter-Coater	AGAR SCIENTIFIC Limited, Essex, UK
Analytical balance BP121S	SARTORIUS AG, Goettingen, Germany
Conical Tubes (50 mL)	EPPENDORF AG, Hamburg, Germany
1181 Copper Tape smooth (12 mm x 16.5 m)	DISTRELEC Gesellschaft m.b.H., Vienna, Austria
Electrically conductive double sided tape with conductive fibers	SHIMADZU, Korneuburg, Austria
Sublimation apparatus	Home-built, TU Wien

Material / Instrument	Purchasing company
DMG Icon® – Caries infiltrant – proximal	DMG Chemisch-Pharmazeutische Fabrik GmbH, Hamburg, Germany
Scotch® Double Sided Tape Dispensered Rolls (12.7 mm x 6.3 m)	3M, Vienna, Austria
IsoMet™ Low Speed Saw (IsoMet 1000; Buehler; IsoMet 15HC, #11-4254, 0.3 mm, precision sectioning blade)	BUEHLER, Lake Bluff, Illinois, USA
MALDI TOF/RTOF instrument ultrafleXtreme™	BRUKER Daltonics GmbH, Bremen, Germany
Micropipettes	EPPENDORF AG, Hamburg, Germany
Microscope SMZ800 Model C-PS with Digital Camera DS-5M and Control Unit DS-L1, NIKON, equipped with KL1500 Electronic light source	SCHOTT Austria GmbH, Vienna, Austria
PathScan Enabler	MEYER Instruments, Houston, TX, USA
Simplicity® UV Water purification system, F2MA54197E	MILLIPORE S.A.S., Molsheim, France
Stainless-steel target	BRUKER Daltonics GmbH, Bremen, Germany
Modified Waters target plate with 6 cavities of different depths (100; 200; 300; 400; 500 and 700 µm)	WATERS Corporation, Milford, MA, USA
Oven (UM 100)	MEMMERT, Schwabach, Germany
Safe-Lock Tubes (0.5 mL; 1.5 mL; 2.0 mL)	EPPENDORF AG, Hamburg, Germany
Ultra-Low Temperature Freezer MDF-U500VX-PE	PANASONIC Healthcare Co., Ltd., Tokyo, Japan
Ultrasonic bath - BANDELIN SONOREX RK 100	BANDELIN electronic GmbH & Co. KG, Berlin, Germany
Vortex-Mixer 524	LABINCO, Breda, The Netherlands

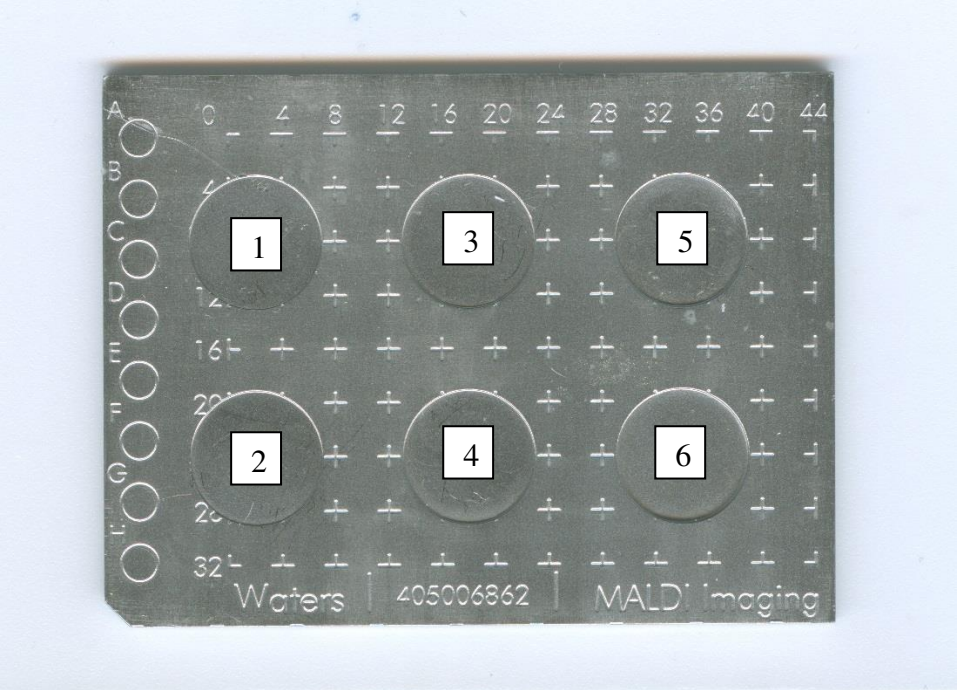

Figure 13 – Measurement on human teeth sections was performed with application of modified Waters target plate with 6 cavities of different depths: (1) 100 µm; (2) 200 µm; (3) 300 µm; (4) 400 µm; (5) 500 µm and (6) 700 µm.

2.1 Sublimation apparatus

Sublimation as matrix application technique was used in one sample preparation procedure on human teeth sections (chapter 2.2.7.2). Components of the home-built sublimation apparatus employed to deposit matrix can be seen in Figure 14.

Firstly, dimensions and weight of modified Waters target plate are measured. Specific amount of matrix is dissolved in defined volume of Acetone/Acetonitrile (7:3, v/v). The amount of matrix depends on favoured thickness of deposited matrix layer. Volume of Acetone/Acetonitrile (7:3, v/v) is determined according to size of entire well. Respectively, volume sufficient for covering the entire area. After pipetting the solution into the preheated matrix well the solvent is allowed to evaporate, inducing crystals formation over the entire well. Modified Waters target plate is mounted onto the sample plate using copper tape smooth (12 mm x 16.5 m; DISTRELEC, Vienna, Austria). The modified Waters target plate is maintained at 10°C by a recirculating fluid cooler using dH_2O/glycol/isopropanol (4:2:0.5, v/v/v). The sublimation apparatus is reassembled, and vacuum is adjusted to 37 mTorr ($5x10^{-2}$ mbar). Sublimation temperature is adjusted according to matrix to be sublimed. Sublimation is preceded until matrix crystals in the well volatilize entirely. Upon

completion of sublimation, the heating is turned off and the device is vented to atmospheric pressure. After sublimation, the target is weighted again to determine average amount of matrix per cm^2.

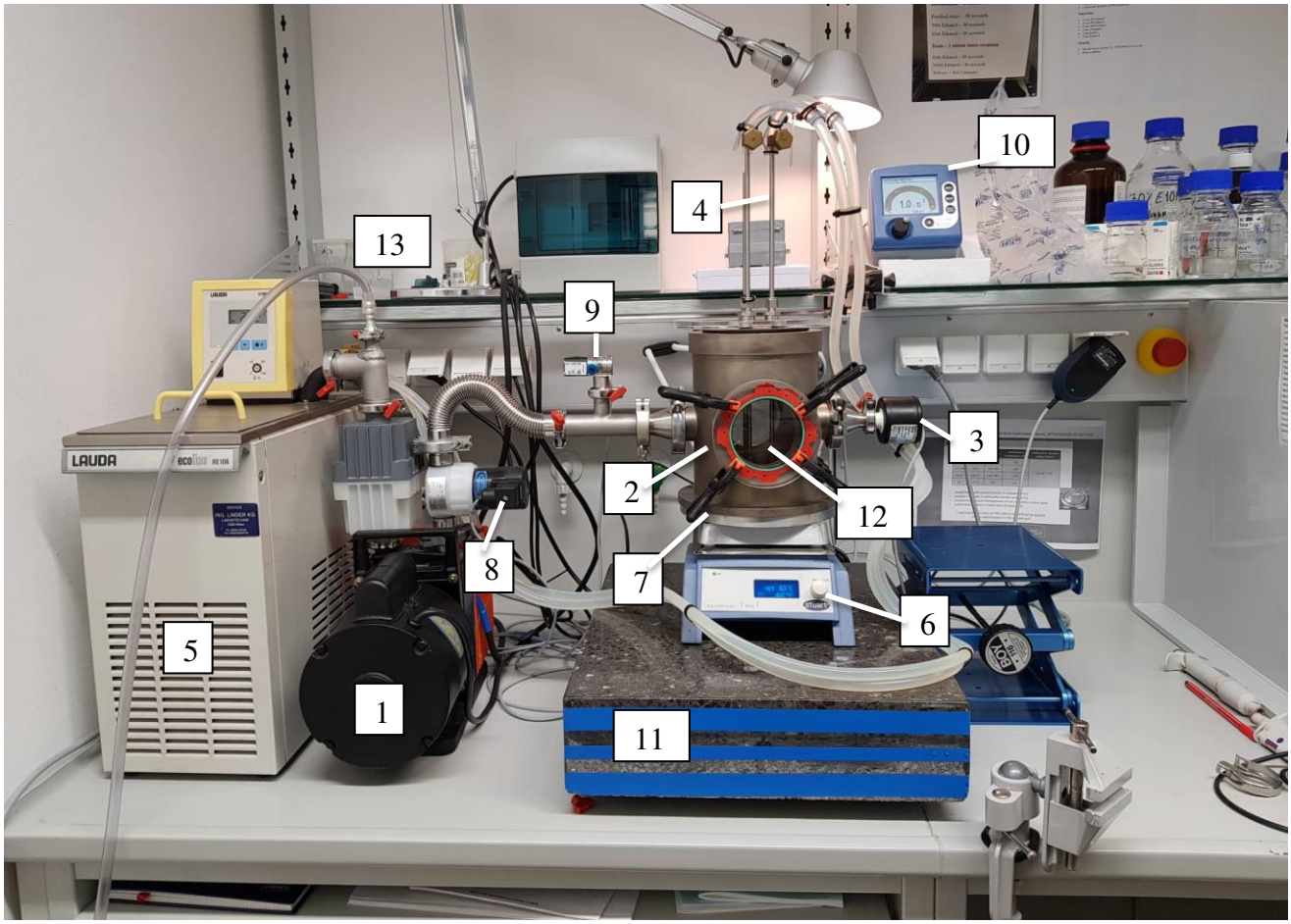

Figure 14 – Setup of the home-built sublimation apparatus for MALDI matrix application: (1) Forevacuum pump; (2) Vacuum-sealed, stainless-steel matrix deposition chamber; (3) Pressure transducer; (4) Modified fluid-cooled condenser; (5) Recirculating fluid, controlled by a cooling unit; (6) Hot-plate; (7) Matrix well and a vacuum control system; (8) Solenoid operated in-line valve; (9) Air admittance valve; (10) Vacuum controller; (11) Granite slab; (12) Removable stainless-steel hollow cylinder; (13) Additional exhaust hose. (Holzlechner, M., MALDI mass spectrometric imaging – Aspects of sample preparation, 2018, p. 68) [20].

2.2 Sample preparation

Chapters 2.2.1 – 2.2.5 involve sample preparation procedures applied in analysis of "*DMG Icon*® – *Caries infiltrant – proximal*", respectively Icon-Dry and Icon-Infiltrant. Chapter 2.2.6 describes

selection and process of cutting of human teeth. Chapter 2.2.7 comprises further manimupation with acquired human teeth sections. At the beginning, process of rinsing and coating of human teeth sections with gold are explained. This chapter is organized into three subchapters, in which three versions of further sample preparation applied on human teeth sections are described.

2.2.1 Icon-Dry pretrial

During optimization of MALDI-TOF-MS preparation, matrices such as 2,5-DHB and Dithranol were tested. Acetonitrile, Toluol and UHQ water were applied in solvent mixtures. AgTFA was applied as cationization reagent in combination with Dithranol. Applied matrices and their concentrations, application of cationization reagent and its concentration, matrix-to-cationization reagent mixing ratios and solvent mixtures can be found in Table 4:

Table 4 – Matrices and their concentrations, application of cationization reagent and its concentration, matrix-to-cationization reagent mixing ratios and solvent mixtures applied in pretrial sample preparation for measurement of Icon-Dry.

Matrix	**Matrix concentration** [mg/mL]	**Cationization reagent:** Yes/No	**Cationization reagent concentration** [mg/mL]	**Matrix-to-cationization reagent mixing ratio**	**Solvent mixture** [µL]
DHB	5.10	No	-	-	Acetonitrile/UHQ water/aquaeous TFA 500/500/1
Dithranol	10	Yes - AgTFA	0.2	50/1	Acetonitrile/Toluol 600/400
Dithranol	10	Yes - AgTFA	0.02	500/1	Acetonitrile/Toluol 600/400

Matrix and cationization reagent (if applied) were weighted in eppendorf tube and dissolved in solvent mixture. Vortex-mixer and ultrasonic bath were used for mixing. First, 0.8 µL Icon-Dry were applied on stainless-steel target (BRUKER Daltonics GmbH, Bremen, Germany) by the pipette tip, dried in ambient conditions. Afterwards, 0.8 µL mixture (comprising matrix and cationization reagent) were added by the same procedure.

2.2.2 Icon-Dry trial

In this sample preparation procedure, Acetonitrile, Toluol and THF were applied as solvent or in solvent mixtures. AgTFA was applied as cationization reagent in all cases. Applied matrix and its concentration, cationization reagent and its concentration, matrix-to-cationization reagent mixing ratios and solvent or solvent mixtures can be found in Table 5.

Table 5 – Matrix and its concentration, cationization reagent and its concentration, matrix-to-cationization reagent mixing ratios and solvent or solvent mixtures applied in trial sample preparation for measurement of Icon-Dry.

Matrix	**Matrix concentration** [mg/mL]	**Cationization reagent**	**Cationization reagent concentration** [mg/mL]	**Matrix-to-cationization reagent mixing ratio**	**Solvent / solvent mixture** [µL]
Dithranol	10	AgTFA	2	5/1	Acetonitrile/Toluol 500/500
Dithranol	10	AgTFA	0.7	15/1	Acetonitrile/Toluol 500/500
Dithranol	10	AgTFA	2	5/1	THF
Dithranol	10	AgTFA	0.7	15/1	THF

Matrix and cationization reagent were weighted in eppendorf tube and dissolved in solvent or solvent mixture. Vortex-mixer and ultrasonic bath were used for mixing. First, 0.8 µL Icon-Dry were applied on stainless-steel target (BRUKER Daltonics GmbH, Bremen, Germany) by the pipette tip, dried in ambient conditions. Afterwards, 0.8 µL mixture (comprising matrix and cationization reagent) were added by the same procedure.

2.2.3 Icon-Dry substitution matrix

As a first option for substitution matrix, THAP was tested. Acetonitrile, Toluol and THF were applied as solvent or in solvent mixtures. AgTFA was applied as cationization reagent in all cases.

Applied matrix and its concentration, cationization reagent and its concentration, matrix-to-cationization reagent mixing ratios and solvent or solvent mixtures can be found in Table 6.

Table 6 – Matrix and its concentration, cationization reagent and its concentration, matrix-to-cationization reagent mixing ratios and solvent or solvent mixtures applied in search for substitution matrix for measurement of Icon-Dry.

Matrix	**Matrix concentration** [mg/mL]	**Cationization reagent**	**Cationization reagent concentration** [mg/mL]	**Matrix-to-cationization reagent mixing ratio**	**Solvent / solvent mixture** [µL]
THAP	10	AgTFA	2	5/1	Acetonitrile/Toluol 500/500
THAP	10	AgTFA	0.7	15/1	Acetonitrile/Toluol 500/500
THAP	10	AgTFA	2	5/1	THF
THAP	10	AgTFA	0.7	15/1	THF

Matrix and cationization reagent were weighted in eppendorf tube, dissolved in solvent or solvent mixture and mixed as in previous two sample preparation procedures. Also, the same steps were performed on stainless-steel targets (BRUKER Daltonics GmbH, Bremen, Germany). 0.8 µL Icon-Dry and 0.8 µL mixture (comprising matrix and cationization reagent) were applied by the pipette tip. Each volume application was followed by drying in ambient conditions.

2.2.4 Icon-Infiltrant pretrial

During this optimization of sample preparation, DCTB as matrix, THF as solvent and NaTFA as cationization reagent were applied in all cases. Two mixtures were prepared. Variation between these two mixtures was in matrix-to-cationization reagent mixing ratio. Applied matrix and its concentration, cationization reagent and its concentration, matrix-to-cationization reagent mixing ratios and solvent can be found in Table 7:

Table 7 – Matrix and its concentration, cationization reagent and its concentration, matrix-to-cationization reagent mixing ratios and solvent applied in pretrial sample preparation for measurement of Icon-Infiltrant.

Matrix	**Matrix concentration** [mg/mL]	**Cationization reagent**	**Cationization reagent concentration** [mg/mL]	**Matrix-to-cationization reagent mixing ratio**	**Solvent**
DCTB	40	NaTFA	0.07	500/1	THF
DCTB	40	NaTFA	0.007	5000/1	THF

Matrix and cationization reagent were weighted in eppendorf tube and dissolved in solvent. Vortex-mixer and ultrasonic bath were used for mixing. First, 0.8 µL Icon-Infiltrant were applied on stainless-steel target (BRUKER Daltonics GmbH, Bremen, Germany) by the pipette tip and dried in vacuum desiccator for 45 minutes. Afterwards, 0.8 µL mixture (comprising matrix and cationization reagent) were added and dried in vacuum dessicator for 45 minutes again.

2.2.5 Icon-Infiltrant trial

In this sample preparation procedure, THF and UHQ water were applied as solvents. NaTFA and NaCl were applied as cationization reagents in the same concentration values. Applied

concentrations of cationization reagents resulted in lower matrix-to-cationization reagent mixing ratio for both. Hence, 4.35:1 for DCTB:NaTFA and 1.87:1 for DCTB:NaCl. Applied matrix and cationization reagents, their concentrations and solvents can be found in Table 8:

Table 8 – Matrix and cationization reagents, their concentrations and solvents applied in trial sample preparation for measurement of Icon-Infiltrant.

Matrix	**Matrix concentration** [mg/mL]	**Matrix solvent**	**Cationization reagent**	**Cationization reagent concentration** [mg/mL]	**Cationization reagent solvent**
DCTB	40	THF	NaTFA	5	THF
DCTB	40	THF	NaCl	5	UHQ water

In both cases, dried-droplet method was applied. Thus, 10 µL matrix solution, 10 µL Icon-Infiltrant and 2.5 µL cationization reagent solution were mixed in eppendorf tube by using vortex-mixer and ultrasonic bath. Afterwards, 0.8 µL were applied directly on stainless-steel target (BRUKER Daltonics GmbH, Bremen, Germany) by the pipette tip and dried in vacuum desiccator for 45 minutes.

2.2.6 Human teeth

The teeth were collected by a dental disposal company (Enretec) located in Velten, Germany. 18 human permanent healthy teeth were selected by Dr. med. dent. Ina Brigitte Ulrich at Danube Private University located in Krems an der Donau, Austria. Only healthy teeth without caries, fillings, and cracks were included in the further experiments. Prior to use, the teeth were carefully cleaned from natural deposits as calculus and soft tissue by means of a dental ultrasonic scaler

(TENEO; Dentsply Sirona, Bensheim, Germany). The teeth were stored in ultra-low temperature freezer at temperature – 70^{0}C immediately after arrival until process of cutting was performed.

Before starting of cutting process, each tooth was fixed to sample holder mechanically to achieve stable position (Figure 15). Subsequently, tooth was cut using IsoMet^{TM} Low Speed Saw (IsoMet 1000; Buehler; IsoMet 15HC, #11-4254, 0.3 mm, precision sectioning blade; Buehler) under continuous manual destilled water cooling. Section thickness was measured by micrometer screw gauge and sections with thickness values suitable for target used (100, 200, 300, 400, 500 and 700 µm) in measurement were chosen only. Tweezers were used to capture the acquired sections in the whole process. These sections were immediately stored in safe-lock tubes or on microscope glass slides inserted to conical tubes depending on size of slice and placed into ultra-low temperature freezer at temperature – 70^{0}C until further use.

Figure 15 – Cutting of human tooth fixed to sample holder. This process was realized under continuous manual destilled water cooling.

2.2.7 Human teeth sections

Each acquired human tooth section used in this study underwent the same procedure of rinsing in solvents and coating with gold.

At first, analysed human teeth sections were removed from ultra-low temperature freezer. The same as during the process of cutting, each section was captured only by the tweezers and rinsed in turns in UHQ water and 2-Propanol. Clean sections were dried in ambient conditions. Clean and dry human teeth sections were fixed to glass slide by applying piece of double sided tape (Scotch®, 12.7 mm x 6.3 m; 3M, Vienna, Austria) and covered with layer of gold. For that purpose, AGAR Gold-Sputter-Coater was used during the period 120 s. Afterwards, gold-covered human teeth sections were gently removed from glass slide and fixed to modified Waters target plate by electrically conductive double sided tape with conductive fibers (SHIMADZU, Korneuburg, Austria).

On analysed human teeth sections were applied three versions of sample preparation, which are explained in subchapters 2.2.7.1 – 2.2.7.3. Depending on concrete sample preparation procedure, Icon-Infiltrant was applied before or after coating with gold.

2.2.7.1 Layer of gold as a solution for electrical conductivity (Version 1)

In this version, human teeth sections (200 and 300 µm) were coated with gold as first. Solutions of matrix and cationization reagent found in Table 9 were prepared. Afterwards, 10 µL matrix solution, 10 µL Icon-Infiltrant and 2.5 µL cationization reagent solution were mixed in eppendorf tube; vortex-mixer and ultrasonic bath were used for mixing.

Table 9 – Matrix and cationization reagent, their concentrations and solvents used in sample preparation of mixture, which was subsequently applied on human teeth sections (200 and 300 µm) in version 1.

Matrix	**Matrix concentration** [mg/mL]	**Matrix solvent**	**Cationization reagent**	**Cationization reagent concentration** [mg/mL]	**Cationization reagent solvent**	**Matrix-to-cationization reagent mixing ratio**
DCTB	40	THF	NaTFA	5	THF	4.35:1

In all cases, 0.8 µL mixture (comprising matrix, Icon-Infiltrant and cationization reagent) were applied directly on gold-coated human teeth sections by the pipette tip and dried in vacuum desiccator for 45 minutes.

2.2.7.2 Matrix sublimation and MS Imaging (Version 2)

2 forms of human teeth sections (200 and 500 µm) were used for analysis in version 2. In first form, Icon-Infiltrant was not applied and human teeth sections were covered with gold. In second form, 0.8 µL Icon-Infiltrant were applied on human teeth sections by the pipette tip and dried in vacuum desiccator for 45 minutes. Afterwards, coating with gold was performed.

The home-built sublimation device was used to sublime DCTB matrix. Dimensions and weight of modified Waters target plate were measured before matrix sublimation. Calculated surface area of modified Waters target plate is 21.98 cm². 25 mg of DCTB matrix were dissolved in 3.8 mL Acetone/Acetonitrile (7:3; v/v). After pipetting the solution into the preheated matrix well (63 °C) the solvent was allowed to evaporate, inducing crystals formation over the entire well. Target was mounted onto the sample plate using copper tape smooth (12 mm x 16.5 m; DISTRELEC, Vienna, Austria). The sample plate was maintained at 10 °C by a recirculating fluid cooler using dH_2O/glycol/isopropanol (4:2:0.5; v/v/v). The sublimation apparatus was reassembled, and vacuum was adjusted to 37 mTorr ($5x10^{-2}$ mbar). Sublimation temperature was adjusted to DCTB matrix

(80 °C). Sublimation was proceded until matrix crystals in the well volatilized entirely (10 min). Upon completion of sublimation, the heating was turned off and the device was vented to atmospheric pressure. After sublimation, the target was weighted again to determine average amount of matrix per cm^2.

2.2.7.3 Icon-Infiltrant under layer of gold and droplet of matrix on the top (Version 3)

This version began with application of 0.8 µL Icon-Infiltrant on human teeth sections (200 and 700 µm) by the pipette tip with subsequent drying in vacuum desiccator for 45 minutes. Afterwards, coating with gold was performed. Matrix solution with parameters found in Table 10 was prepared. No cationization reagent was applied. Vortex-mixer and ultrasonic bath were used for mixing.

Table 10 – Matrix, its concentration and solvent used in sample preparation of solution, which was subsequently applied on human teeth sections in version 3.

Matrix	**Matrix concentration** [mg/mL]	**Solvent**
DCTB	40	THF

At last, 0.8 µL of this matrix solution were applied by the pipette tip on human teeth sections and dried in ambient conditions.

2.3 Data acquisition

MS and MSI spectra were acquired on MALDI TOF/RTOF instrument (ultrafleXtreme™), equipped with a 2 kHz Smartbeam™ laser (355 nm) and operated with flexControl v3.4 (all BRUKER Daltonics GmbH, Bremen, Germany). All spectra were measured in positive ion mode. Information about accumulation of selected spectra, if measurement was performed in reflectron or

linear mode can be found undear each spectrum in this thesis. Applied laser power can be found in the text discussing obtained data. The laser power or laser power range for each sample was defined by the ability to obtain mass signal. Obtained spectra were processed in flexAnalysis and mMass software. In MS Imaging, data acquisition and image representation were carried out using flexImaging software v3.0. In MS Imaging, 100 µm raster width was applied and smartbeam paramater was set to medium. Regions of measurement were chosen manually. Thus, shooting of laser on the whole human tooth section surface area in order to observe distribution of matrix and Icon-Infiltrant. MS Imaging was performed on surface area of modified Waters target plate too. This served for comparison, how sublimed matrix is distributed on different surfaces.

Peptide calibration Mix 4 (Proteomix) was used as calibration standard for external calibration in the mass range *m/z* 500 – 3500 Da. This calibration standard covers mass range of interest. Matrix solution 10 mg α-CHCA in 1.0 mL of 50% Acetonitrile, 50% of UHQ Water and 0.1% TFA was prepared according to MALDI matrix preparation protocol [49]. Peptide calibration Mix 4 (Proteomix) was diluted in 1:10 stock solution-to-matrix solution mixing ratio. 1 µL of this mixture were spotted on adjacent target spot on stainless-steel target (BRUKER Daltonics GmbH, Bremen, Germany) or modified Waters target plate before each measurement. Measurement of peptides with known masses resulted in spectrum used for calibration.

3. Results and discussion

3.1 Icon-Dry pretrial

This chapter presents results obtained from preliminary measurement of Icon-Dry. Material safety data sheet of Icon-Dry states that Icon-Dry consists of 99% Ethanol [50]. As it was already explained in chapter 1.2.1, in MALDI analysis, solvent evaporation takes place after the sample solution is deposited onto the probe. Therefore no signals related to Icon-Dry were expected.

Icon-Dry syringe is polymer-based material [51] and its release into syringe content might occur. Based on these assumptions, approach commonly used in MALDI-TOF-MS analysis of synthetic polymers was chosen in preliminary measurement. In other words, matrix and cationization reagent used for analysis of synthetic polymers were applied.

In case of synthetic polymers, it is very important to select an appropriate matrix in order to obtain a good mass spectrum, because synthetic polymers have a variety of molecular structures and

different polarities ranging from hydrophilic (e.g., Polyethylene Glycol) to relatively hydrophobic (e.g., Polystyrene). For example, 2,5-DHB and Dithranol matrices are recommended as matrices for Polyethylene Glycol, Polystyrene and Polyamide, respectively [52].

Polymers with high proton affinity can be protonated by most matrices (which frequently contain carboxylic acid groups), but for other polymers, a cationization reagent is required [53]. To find out, if release of syringe material into syringe content occurs, matrices such as 2,5-DHB and Dithranol were tested in preliminary measurement of Icon-Dry. The selection of an appropriate matrix with similar solubility parameters as the polymer analyte is critical to obtain high quality spectra [53]. For that reason, water soluble 2,5-DHB matrix and non-water soluble Dithranol matrix were tested.

No spectra were obtained with application of 2,5-DHB in both linear and reflectron mode. However, reflectron mode showed meaningful results for Dithranol.

Figure 16 shows spectrum produced with application of Dithranol matrix in mass range 150-3500 Da. 10 mg Dithranol matrix and 0.2 mg AgTFA cationization reagent were dissolved in Acetonitrile/Toluol (600/400) µL resulting in matrix-to-cationization reagent mixing ratio 50:1. Polymers are mixtures of oligomers differing in mass by the mass of the repeating units. Therefore, in polymer mass spectra, distributions of molecular ions are detected, rather than a single type of a molecular ion [54]. In first obtained spectrum, it can be clearly seen the distribution of oligomers in mass range 1300-3500 Da that define the polymer. From the masses of adjacent ion peaks, the mass of the repeat unit can be measured. $\Delta m/z$ of adjacent ion peaks can be expressed as $\Delta m/z$ 74.16 ± 0.45. This value represents mean value ± standard deviation calculated from all $\Delta m/z$ of adjacent ion peaks defining the polymer. In this spectrum, m/z of most abundant peak is 1441.448. From this value, chain length of most abundant peak 19 can be determined. This number was obtained as division of most abundant peak m/z value by mean value and was rounded to the nearest one.

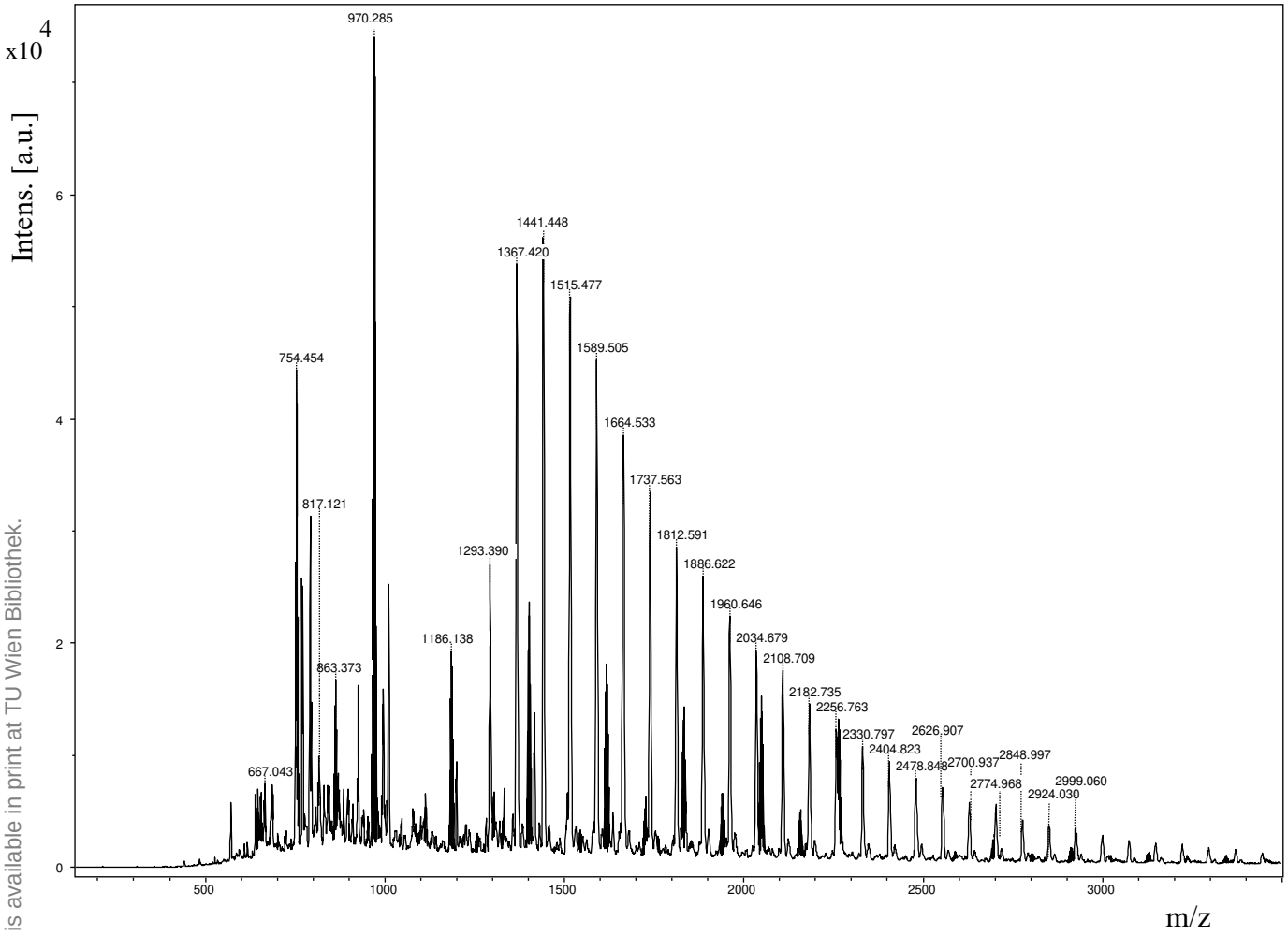

Figure 16 – MALDI MS spectrum of 0.8 µL Icon-Dry covered with 0.8 µL matrix (10 mg Dithranol/mL Acetonitrile/Toluol (600/400) µL mixed with AgTFA cationization reagent 0.2 mg/mL at ratio of 50:1), accumulation of 2000 selected spectra, measured in reflectron mode.

Sample preparation procedure for measurement resulting in spectrum in Figure 17 was the same as in previous case, except of matrix-to-cationization reagent mixing ratio. In this case, matrix-to-cationization reagent mixing ratio 500:1 was applied and influence of alteration of this parameter was to be observed. Thus, 10 mg Dithranol and 0.02 mg AgTFA cationization reagent were dissolved in Acetonitrile/Toluol (600/400) µL resulting in matrix-to-cationization reagent mixing ratio 500:1. Mass spectrum in Figure 17 shows the distribution of oligomers in mass range 1300-3500 Da that define the polymer. $\Delta m/z$ of adjacent ion peaks can be expressed as $\Delta m/z$ 74.22 ± 0.39. In this spectrum, m/z of most abundant peak is 1441.478. From this value, chain length of most abundant peak 19 can be determined.

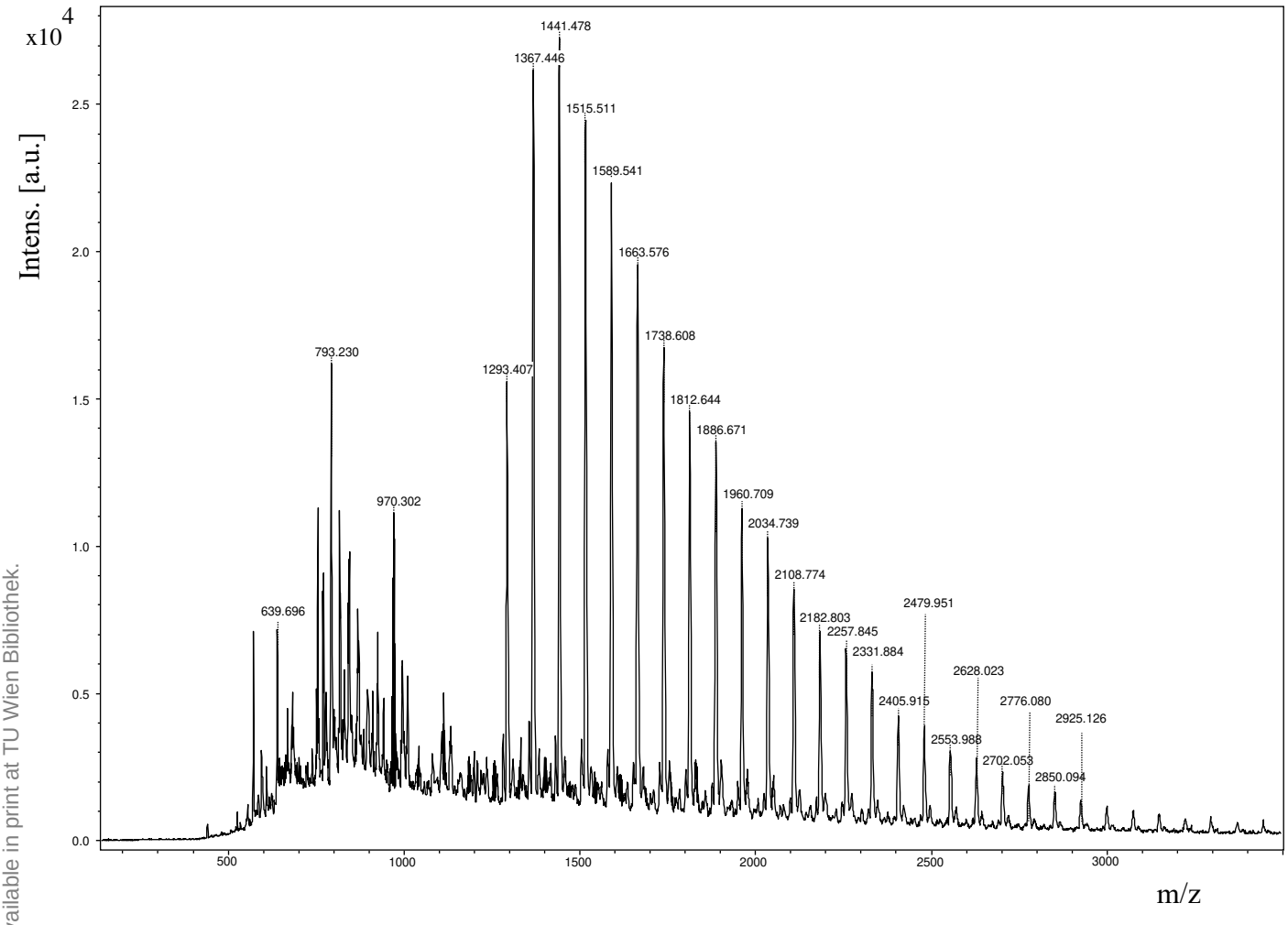

Figure 17 – MALDI MS spectrum of 0.8 µL Icon-Dry covered with 0.8 µL matrix (10 mg Dithranol/mL Acetonitrile/Toluol (600/400) µL mixed with AgTFA cationization reagent 0.02 mg/mL at ratio of 500:1), accumulation of 2000 selected spectra, measured in reflectron mode.

Laser power 60-90% was applied in both cases. Comparing these spectra, it can be concluded that matrix-to-cationization reagent mixing ratio 50:1 resulted in higher intensity of ions peaks. Both spectra show distribution of oligomers in mass range 1300-3500 Da. The *m/z* values of most abundant peaks differ only in decimals, *m/z* 1441.448 Da (Figure 16) and *m/z* 1441.478 Da (Figure 17). The same can be stated for calculated mean values and standard deviations. Based on this, the same value of chain length of most abundant peaks was obtained. Peaks *m/z* 970.285 Da in Figure 16 and *m/z* 970.302 Da in Figure 17 can be seen. As this *m/z* value appeared in both spectra, it may be assumed that it belongs to polymer structure. What more can be observed, ion peaks *m/z* 667.043 Da, *m/z* 754.454 Da, *m/z* 817.121 Da, *m/z* 863.373 Da and *m/z* 1186.138 Da were detected in Figure 16. In Figure 17, *m/z* 639.696 Da and *m/z* 793.230 Da were detected. These ion peaks may result

from formation of clusters. However, further measurements are necessary to prove previous statements.

According to obtained results in preliminary measurement, further measurements were performed in reflectron mode and Dithranol as matrix at concentration value 10 mg/mL with AgTFA as cationization reagent were applied.

3.2 Icon-Dry trial

Second measurement focused on characterization of Icon-Dry syringe content was performed. Results obtained in preliminary measurement of Icon-Dry (chapter 3.1) were considered in choosing further conditions. Thus, 10 mg Dithranol/mL, AgTFA as cationization reagent and combination of solvents Acetonitrile/Toluol (1:1; v/v) were applied as in previous chapter. Moreover, coming out of Dithranol matrix preparation protocol for non-water soluble organic and aromatic polymer samples [55], THF was applied as next solvent. 5:1 and 15:1 matrix-to-cationization reagent mixing ratios were used, resulting in 2 mg/mL and 0.7 mg/mL concentration values of AgTFA. Laser power 50-60% was applied to obtain each spectrum presented in this chapter.

In this measurement, influence of applying different solvent and lower matrix-to-cationization reagent mixing ratios were to be observed.

Spectra obtained in this measurement can be seen in Figure 18 – 21.

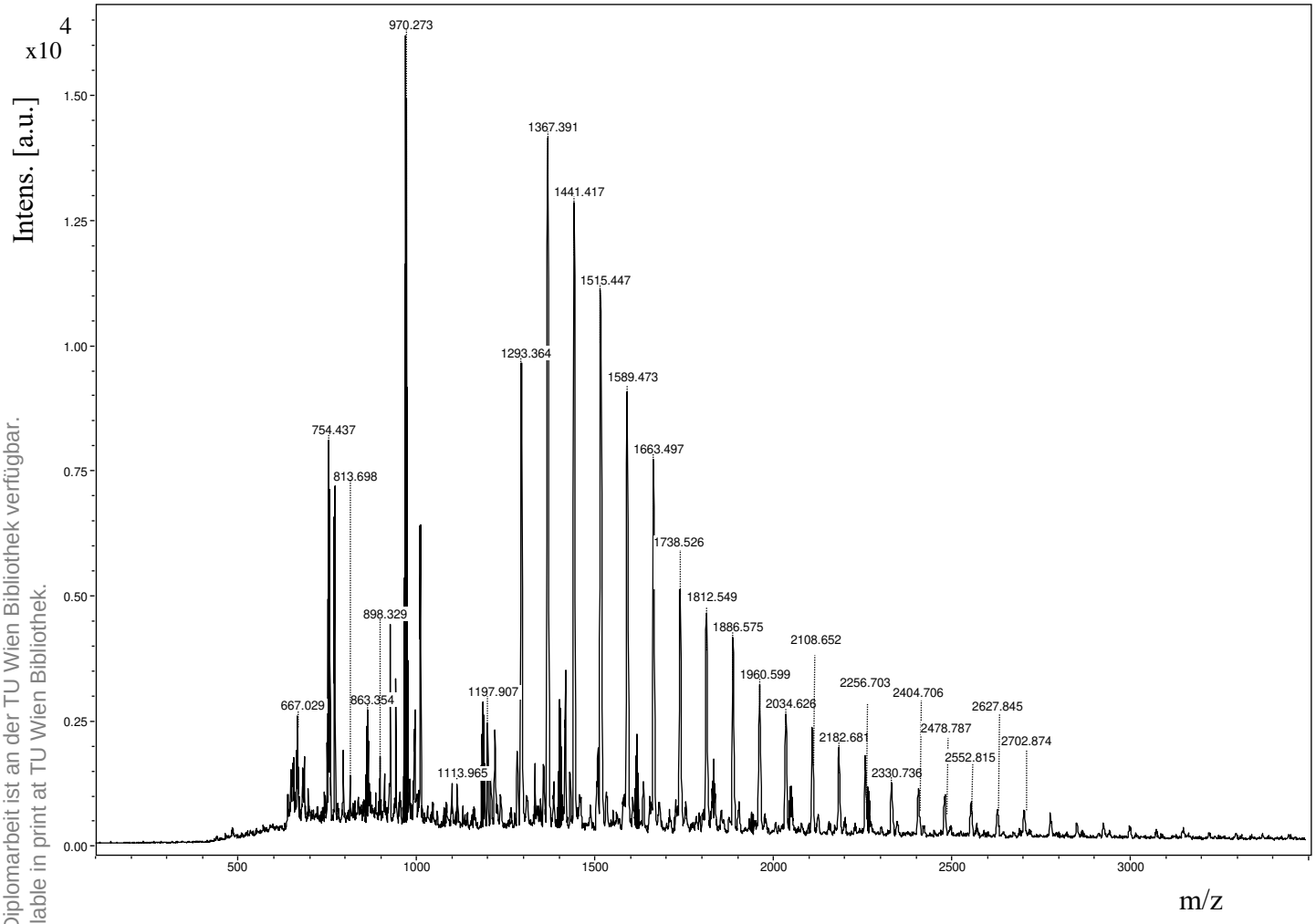

Figure 18 – MALDI MS spectrum of 0.8 µL Icon-Dry covered with 0.8 µL matrix (10 mg Dithranol/mL THF mixed with AgTFA cationization reagent 2 mg/mL at ratio of 5:1), accumulation of 2200 selected spectra, measured in reflectron mode.

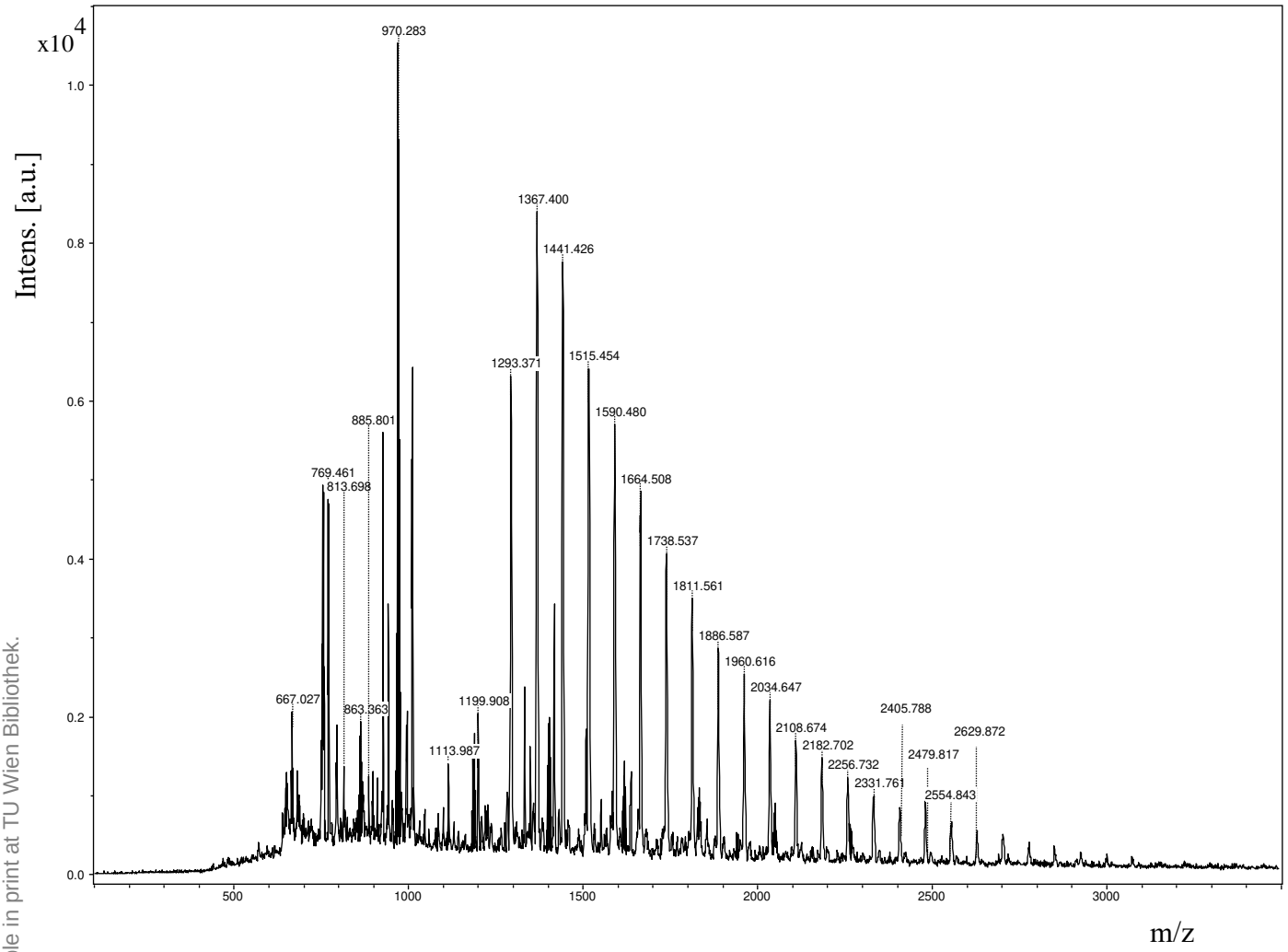

Figure 19 – MALDI MS spectrum of 0.8 µL Icon-Dry covered with 0.8 µL matrix (10 mg Dithranol/mL THF mixed with AgTFA cationization reagent 0.7 mg/mL at ratio of 15:1), accumulation of 2000 selected spectra, measured in reflectron mode.

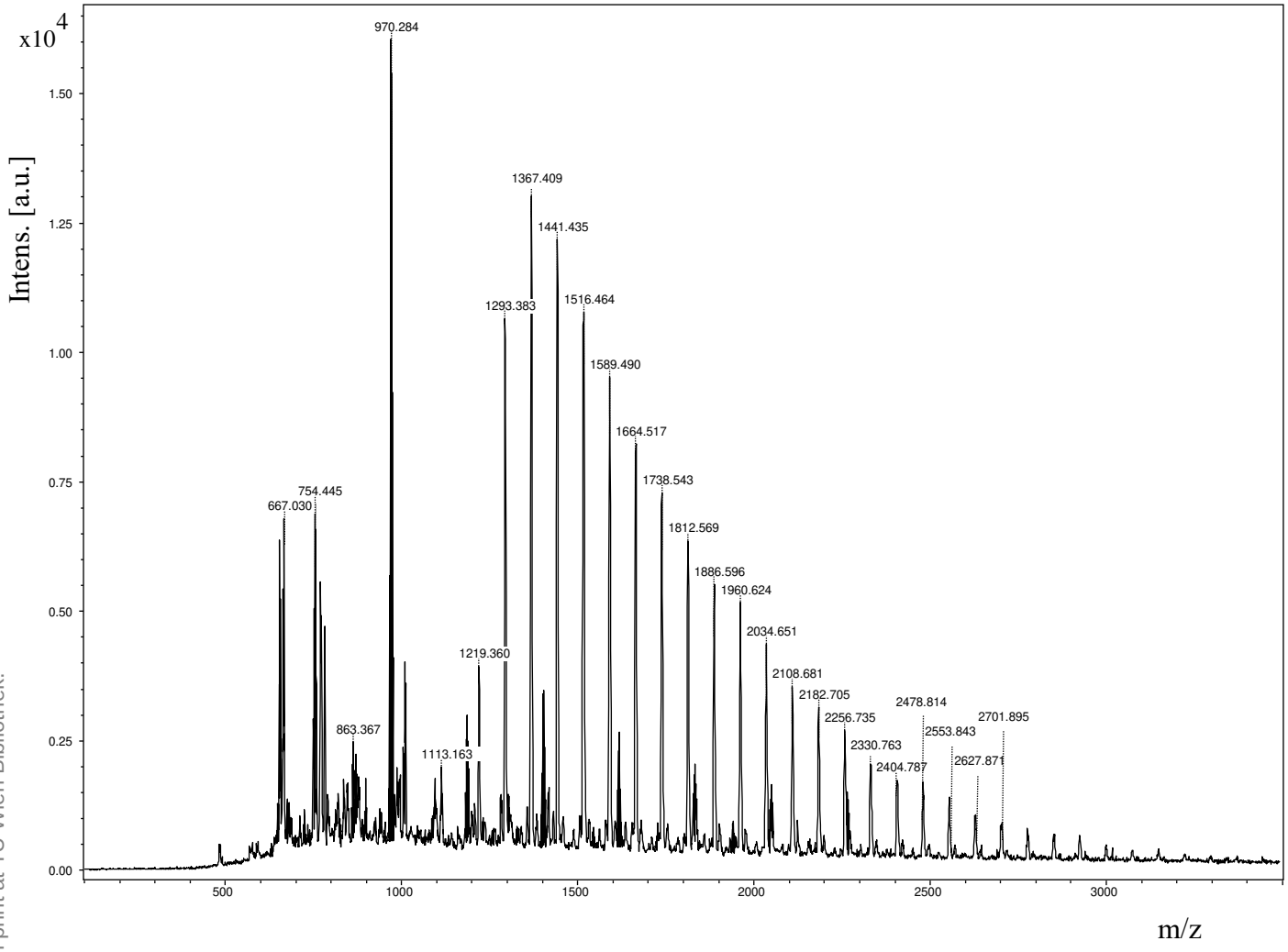

Figure 20 – MALDI MS spectrum of 0.8 µL Icon-Dry covered with 0.8 µL matrix (10 mg Dithranol/mL Acetonitrile/Toluol (500/500) µL mixed with AgTFA cationization reagent 2 mg/mL at ratio of 5:1), accumulation of 1900 selected spectra, measured in reflectron mode.

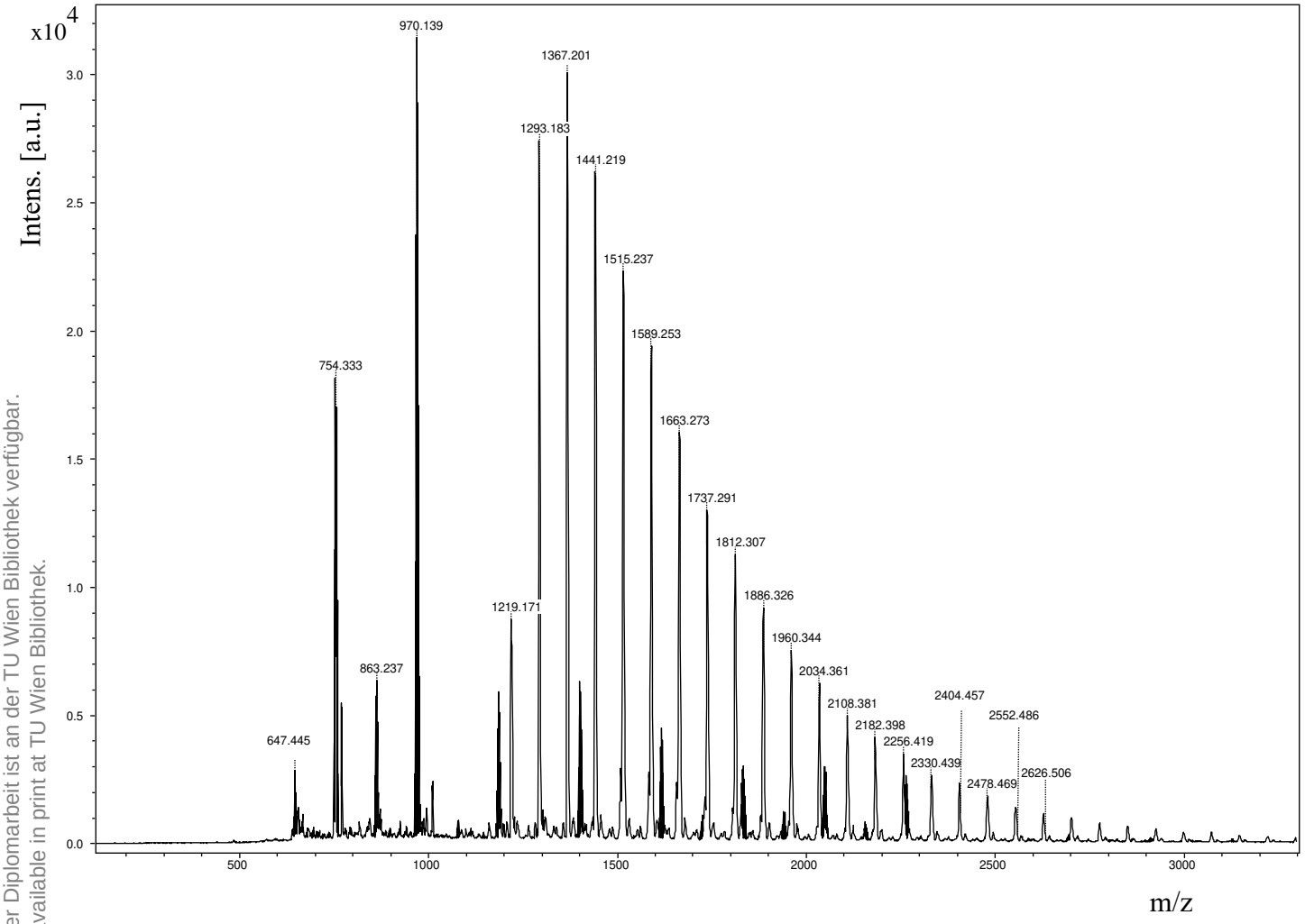

Figure 21 – MALDI MS spectrum of 0.8 µL Icon-Dry covered with 0.8 µL matrix (10 mg Dithranol/mL Acetonitrile/Toluol (500/500) µL mixed with AgTFA cationization reagent 0.7 mg/mL at ratio of 15:1), accumulation of 1900 selected spectra, measured in reflectron mode.

In all 4 spectra, distribution of oligomers in mass range 1200-3000 Da can be observed. These spectra confirm the presence of polymer in Icon-Dry syringe content detected in preliminary measurement of Icon-Dry. The *m/z* values of most abundant peaks are 1367.391 Da, 1367.400 Da, 1367.409 Da and 1367.201 Da. Δ*m/z* of adjacent ion peaks can be expressed as Δ*m/z* 74.24 ± 0.52 Da for Figure 18; Δ*m/z* 74.25 ± 0.53 Da for Figure 19; Δ*m/z* 74.13 ± 0.45 Da for Figure 20 and Δ*m/z* 74.07 ± 0.23 Da for Figure 21. Values of most abundant peaks result in chain length 18 for all spectra.

Moreover, *m/z* 667.029 Da; *m/z* 754.437 Da; *m/z* 813.698 Da; *m/z* 863.354 Da; *m/z* 898.329 Da; *m/z* 970.273 Da; *m/z* 1113.965 Da and *m/z* 1197.907 Da were identified in Figure 18. The *m/z* 667.027 Da; *m/z* 769.461 Da; *m/z* 813.698 Da; *m/z* 863.363 Da; *m/z* 885.801 Da; *m/z* 970.283 Da; *m/z*

1113.987 Da and *m/z* 1199.908 Da were identified in Figure 19. The *m/z* 667.030 Da; *m/z* 754.445 Da; *m/z* 863.367 Da; *m/z* 970.284 Da and *m/z* 1113.163 Da were identified in Figure 20. The *m/z* 647.445 Da; *m/z* 754.333 Da; *m/z* 863.237 Da and *m/z* 970.139 Da were identified in Figure 21. The *m/z* values 970.273 Da (Figure 18), 970.283 Da (Figure 19), 970.284 Da (Figure 20), 970.139 Da (Figure 21) belong to residual mass of polymer, as it was assumed in preliminary measurement of Icon-Dry. The rest ions peaks may result from the formation of clusters, as combination of analyte, matrix and silver ion. Different matrix preparations with altered solvents and concentrations of cationization reagents can lead to different cluster peaks.

Comparing the solvents, following observations can be reported. Application of THF solvent in both matrix-to-cationization reagent mixing ratios resulted in lower intensity of ion peaks. Obtained intensities reached lower values, even though more selected spectra were accumulated (spectrum in Figure 19 – 2000; spectrum in Figure 18 – 2200). In terms of intensity, the combination of solvents Acetonitrile/Toluol (1:1; v/v) and matrix-to-cationization reagent mixing ratio 15:1 proved to be suitably chosen parameters.

To sum up, spectra in Figure 18 – 21 showed distribution of oligomers in the same mass range 1200-3000 Da. Most abundant peak *m/z* values, calculated mean values and standard deviations differed only in decimals. Ion peak of assumed residual mass of polymer was detected in each spectrum.

Comparing spectra of previous and this chapter, different most abundant peak *m/z* values were obtained. Mass range of distribution of oligomers in previous chapter reached upper value 3500 Da, in this chapter 3000 Da. Explanation for that may be that higher matrix-to-cationization mixing ratio leads to shifting in higher mass range. Thus, matrix is more critical than the cationization reagent.

Sample preparation procedure for characterization of Icon-Dry syringe content was proposed. Thus, 10 mg Dithranol/mL and 0.7 mg AgTFA /mL (15:1 matrix-to-cationization reagent mixing ratio) dissolved in mixture of solvents Acetonitrile/Toluol (1:1; v/v) were determined as optimal conditions.

3.3 Icon-Dry substitution matrix

Due to fact that Dithranol with required purity ≥ 98.0% for MALDI analysis has been discontinued by the vendor, an appropriate alternative matrix had to be found. THAP matrix was tested as a first option applying identical conditions in sample preparation as in chapter 3.2. Hence, THAP matrix with concentration 10 mg/mL and AgTFA as cationization reagent. 5:1 and 15:1 matrix-to-cationization reagent mixing ratios were applied with THF as solvent and mixture of solvents Acetonitrile/Toluol (1:1; v/v). The aim of this measurement was to find out, if THAP can be suitable as matrix for measuring Icon-Dry syringe content too. Moreover, if THAP proves to be suitable, variation of matrix-to-cationization reagent mixing ratio and solvents was to be observed in obtained spectra.

Spectra in Figures 22 – 25 show one distribution of oligomers in mass range 1200-3000 Da. This mass range of polymer distribution was also observed with Dithranol matrix in previous chapter, where the same conditions for solvents and matrix-to-cationization reagent mixing ratios were applied.

Hence, these spectra confirm the presence of polymer detected in measurement of Icon-Dry syringe content with Dithranol matrix. The *m/z* values of most abundant peaks are 1367.245 Da (Figure 22), 1367.240 Da (Figure 23), 1367.328 Da (Figure 24) and 1367.321 Da (Figure 25). Δ*m/z* of adjacent ion peaks can be expressed as Δ*m/z* 74.07 ± 0.22 Da for Figure 22; Δ*m/z* 74.30 ± 0.56 Da for Figure 23; Δ*m/z* 74.17 ± 0.47 Da for Figure 24 and Δ*m/z* 74.09 ± 0.25 Da for Figure 25. Values of most abundant peaks result in chain length 18 for all spectra. Laser power applied in this measurement was 80%.

Analysis of *m/z* values occurring in spectra of this chapter resulted in following observations. The *m/z* values 970.166 Da (Figure 22), 970.170 Da (Figure 23), 970.213 Da (Figure 24) and 970.301 Da (Figure 25) were identified. As it was already concluded from spectra with Dithranol matrix, these ion peaks belong to residual mass of polymer. The rest of ion peaks occurring in mass range 300-1200 Da may result again from the formation of clusters, as combination of analyte, matrix and silver ion.

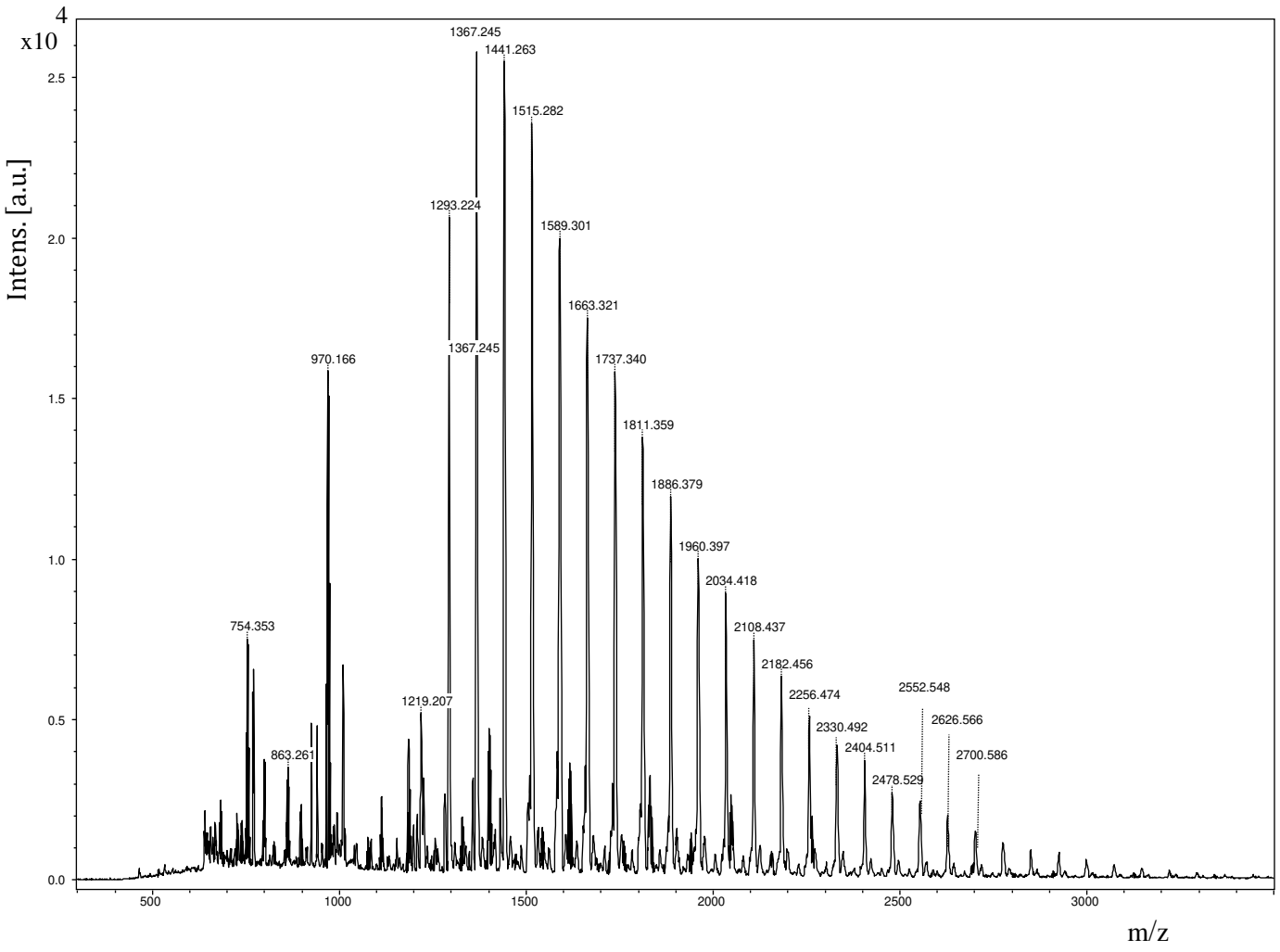

Figure 22 – MALDI MS spectrum of 0.8 µL Icon-Dry covered with 0.8 µL matrix (10 mg THAP/mL THF mixed with AgTFA cationization reagent 2 mg/mL at ratio of 5:1), accumulation of 400 selected spectra, measured in reflectron mode.

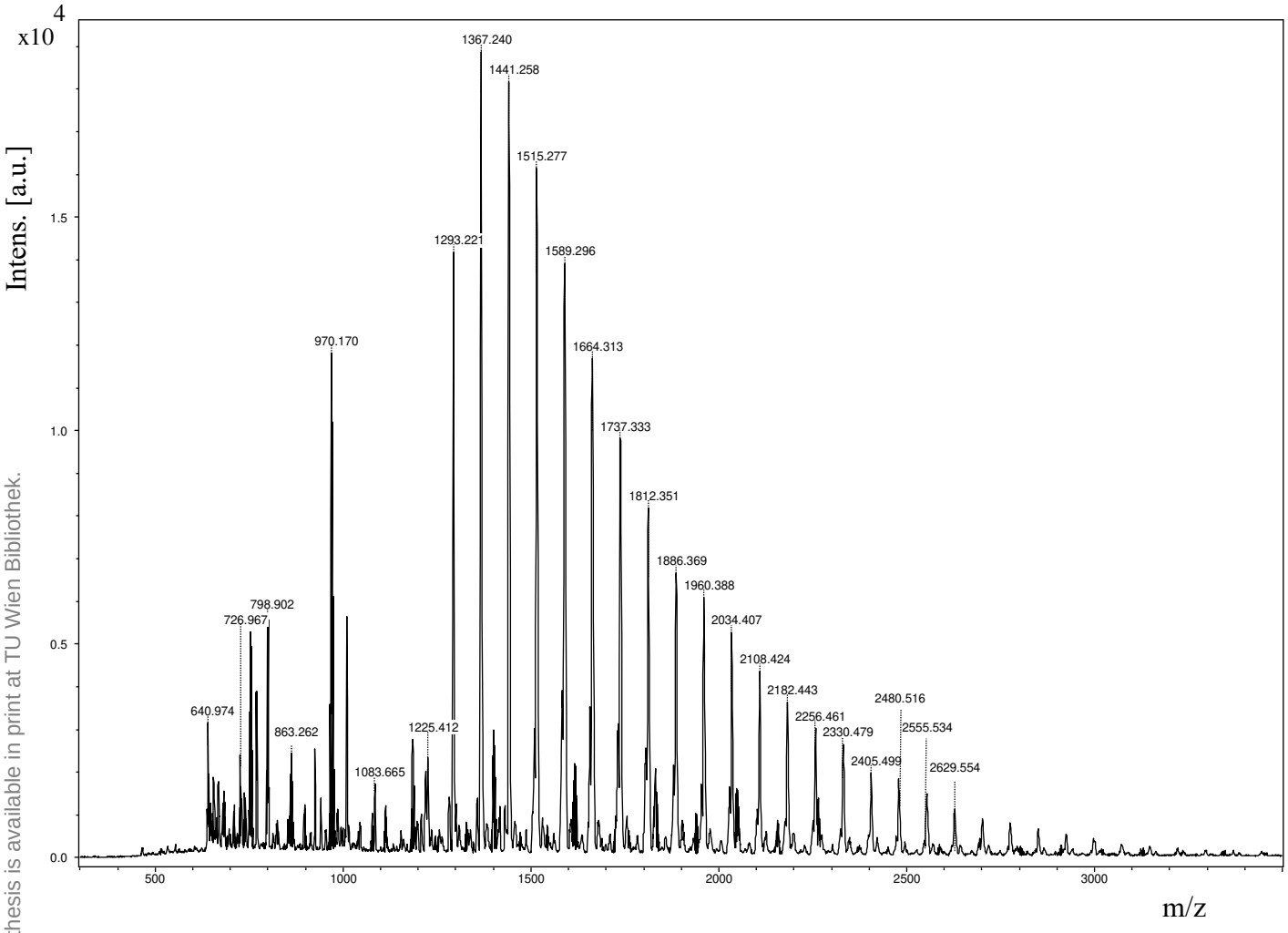

Figure 23 – MALDI MS spectrum of 0.8 µL Icon-Dry covered with 0.8 µL matrix (10 mg THAP/mL THF mixed with AgTFA cationization reagent 0.7 mg/mL at ratio of 15:1), accumulation of 600 selected spectra, measured in reflectron mode.

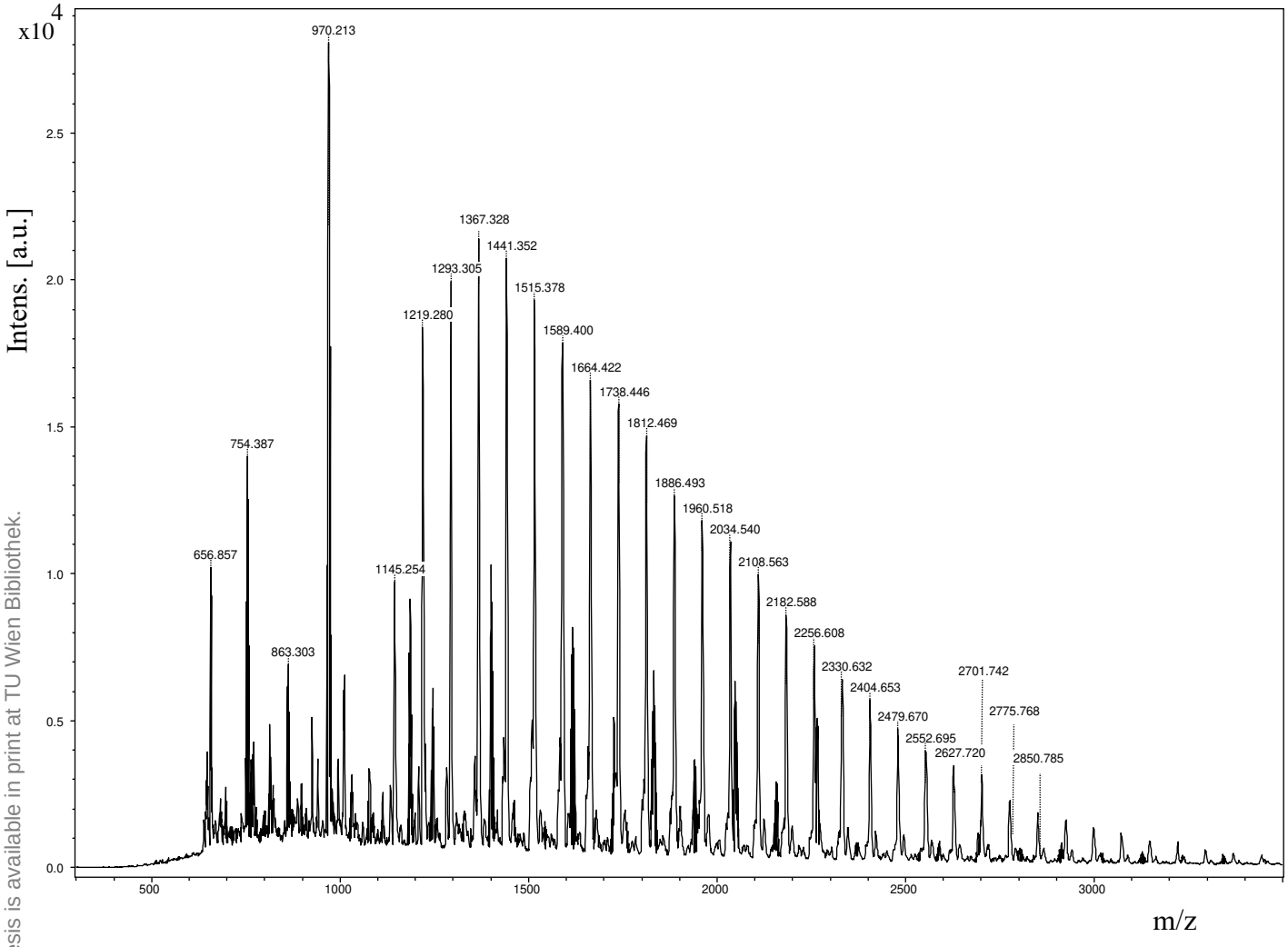

Figure 24 – MALDI MS spectrum of 0.8 µL Icon-Dry covered with 0.8 µL matrix (10 mg THAP/mL Acetonitrile/Toluol (500/500) µL mixed with AgTFA cationization reagent 2 mg/mL at ratio of 5:1), accumulation of 400 selected spectra, measured in reflectron mode.

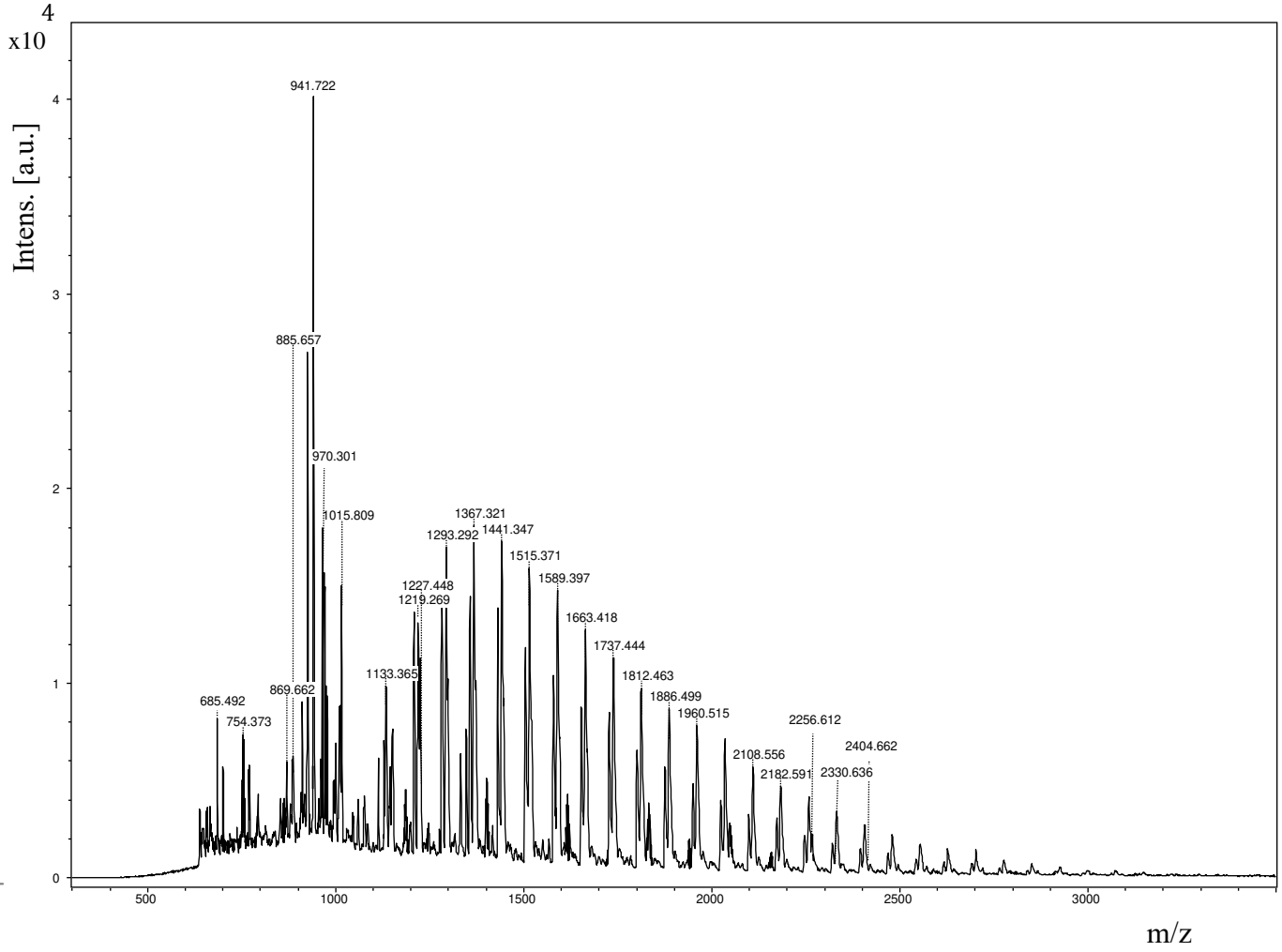

Figure 25 – MALDI MS spectrum of 0.8 µL Icon-Dry covered with 0.8 µL matrix (10 mg THAP/mL Acetonitrile/Toluol (500/500) µL mixed with AgTFA cationization reagent 0.7 mg/mL at ratio of 15:1), accumulation of 500 selected spectra, measured in reflectron mode.

Beginning with highest acquired intensity, mixture of solvents Acetonitrile/Toluol (1:1; v/v) and matrix-to-cationization mixing ratio 15:1 parameters proved to be the most effective. This confirms result obtained with application of Dithranol matrix.

Considering both – intensity and signal-to-noise ratio, it comes to the conclusion that THF as a solvent and 5:1 matrix-to-cationization mixing ratio are optimal conditions for measurement of Icon-Dry syringe content with THAP matrix. Figure 23 shows spectrum obtained under these conditions, S/N of most abundant peak is 144.

To sum up, spectra in Figure 22 – 25 showed distribution of oligomers in the same mass range 1200-3000 Da as in chapter 3.2. Most abundant peak *m/z* values, calculated mean values and

standard deviations were varying only in decimals. Reproducible analytical results were obtained with another matrix.

Sample preparation procedure for characterization of Icon-Dry syringe content with another matrix was proposed. 10 mg THAP/mL and 2 mg AgTFA/mL (5:1 matrix-to-cationization reagent mixing ratio), both dissolved in THF were determined as optimal conditions.

3.4 Icon-Infiltrant pretrial

Objective of this study was to characterize Icon-Infiltrant by applying MALDI-TOF-MS. Results of preliminary measurement of Icon-Infiltrant syringe content will be discussed in this chapter.

First of all, determination of suitable matrix for measurement of Icon-Infiltrant was matter of interest. Considering Icon-Infiltrant composition – Triethylene glycol dimethacrylate (TEDMA) (70 – 95)% and Camphoro Quinone (< 2.5%), DCTB matrix was applied as a first option [56]. DCTB is a nonpolar, aprotic matrix and has been considered as an excellent matrix for MALDI of many types of synthetic compounds [57-59].

Subsequently, different matrix-to-cationization reagent mixing ratios were to be observed in obtained spectra. For that purpose, 500:1 and 5000:1 matrix-to-cationization reagent mixing ratios were tested. Concentration of DCTB 40 mg/mL, THF as solvent and NaTFA as cationization reagent were applied in both cases.

No meaningful signals were obtained in reflectron mode for both applied molar ratios. However, molar ratio 500:1 produced spectrum measured in linear mode that can be seen in Figure 26. This spectrum was obtained at laser power 77%.

For spectrum in Figure 26, 3 distributions of oligomers in mass range 400-700 Da, 700-1100 Da and 1100-1500 Da can be identified. The *m/z* values of most abundant peaks are 538.925 Da, 870.161 Da and 1200.199 Da. $\Delta m/z$ of adjacent ion peaks can be expressed as $\Delta m/z$ 44.06 ± 0.07 Da for first distribution of oligomers; $\Delta m/z$ 44.01 ± 0.02 Da for second distribution of oligomers and $\Delta m/z$ 44.17 ± 0.36 Da for third distribution of oligomers. Values of most abundant peaks result in chain length 12 for first distribution of oligomers; 20 for second distribution of oligomers and 27 for third distribution of oligomers.

Moreover, the *m/z* 97.889 Da; *m/z* 276.461 Da and *m/z* 309.480 Da were detected.

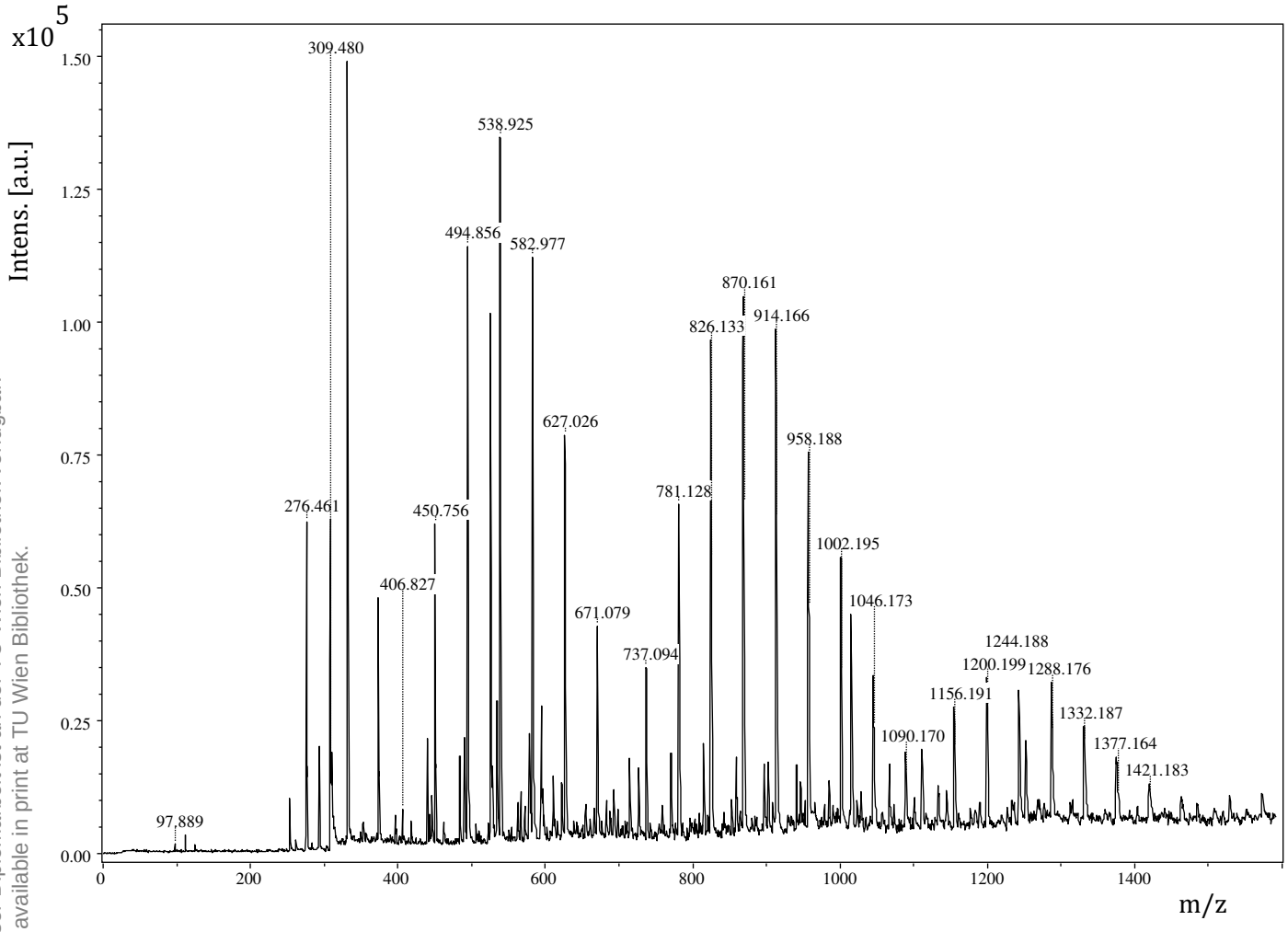

Figure 26 – MALDI MS spectrum of 0.8 µL Icon-Infiltrant covered with 0.8 µL matrix (40 mg DCTB/mL THF mixed with NaTFA cationization reagent 0.07 mg/mL at ratio of 500:1), accumulation of 1800 selected spectra, measured in linear mode.

3.5 Icon-Infiltrant trial

For further analysis of Icon-Infiltrant syringe content, parameters were proposed according to results obtained in Icon-Infiltrant preliminary measurement (chapter 3.4). As concentration 40 mg/mL DCTB matrix and application of THF solvent resulted in meaningful signals, these conditions were not altered. Lower matrix-to-cationization reagent mixing ratio than 500:1 and difference by applying two different cationization reagents were to be observed in obtained spectra. Hence, 4.35:1 for DCTB:NaTFA and 1.87:1 for DCTB:NaCl. In this measurement, matrix, Icon-

Infiltrant and cationization reagent were mixed in 4:4:1 volume ratio in an eppendorf tube according to DCTB matrix MALDI preparation protocol [60]. This method is known as dried-droplet method and has remained the preferred sample preparation method in the MALDI community [61]. Laser power 85-88% was applied in both spectra. Spectra obtained in this measurement can be seen in Figures 27 and 28.

Spectrum obtained with application of NaTFA as cationization reagent resulted in 4 distributions of oligomers in mass range 400-700 Da, 700-1100 Da, 1100-1500 Da and 1500-1800 Da. Spectrum obtained with application of NaCl as cationization reagent resulted in 3 distributions of oligomers in in the same mass ranges. Even though there is presence of certain peaks in mass range 1500-1800 Da, it can not be clearly stated that NaCl resulted in fourth distribution of oligomers.

For Figure 27, *m/z* values of most abundant peaks are 540.130 Da, 870.340 Da, 1179.411 Da and 1563.353 Da. Δ*m/z* of adjacent ion peaks can be expressed as Δ*m/z* 44.26 ± 0.41 Da for first distribution of oligomers; Δ*m/z* 44.14 ± 0.33 Da for second distribution of oligomers; Δ*m/z* 44.03 ± 0.03 Da for third distribution of oligomers and Δ*m/z* 44.03 ± 0.01 Da for fourth distribution of oligomers. Values of most abundant peaks result in chain length 12 for first distribution of oligomers; 20 for second distribution of oligomers; 27 for third distribution of oligomers and 36 for fourth distribution of oligomers. Moreover, *m/z* 125.224 Da; *m/z* 205.286 Da; *m/z* 276.690 Da; *m/z* 331.814 Da and *m/z* 373.892 Da were identified.

Data obtained from spectrum in Figure 28, *m/z* values of most abundant peaks are 539.119 Da, 870.313 Da and 1200.268 Da. Δ*m/z* of adjacent ion peaks can be expressed as Δ*m/z* 44.05 ± 0.01 Da for first distribution of oligomers; Δ*m/z* 44.00 ± 0.04 Da for second distribution of oligomers and Δ*m/z* 43.99 ± 0.05 Da for third distribution of oligomers. Values of most abundant peaks result in chain length 12 for first distribution of oligomers; 20 for second distribution of oligomers and 27 for third distribution of oligomers. Except of polymer distributions, *m/z* 47.040 Da; *m/z* 98.064 Da; *m/z* 177.709 Da; *m/z* 276.678 Da; *m/z* 331.818 Da and *m/z* 373.909 Da were detected.

Application of NaTFA resulted in higher intensity. Better signal-to-noise ratio was achieved with NaCl. S/N values for most abundant peaks of this spectrum are 80 (*m/z* 539.119 Da), 27 (*m/z* 870.313 Da) and 13 (*m/z* 1200.268 Da).

Comparing *m/z* values between spectra in Figures 26 – 28, it can be observed that *m/z* 276.461 Da (Figure 26); *m/z* 276.690 Da (Figure 27) and *m/z* 276.678 Da (Figure 28) were detected. Therefore it can be assumed that this peak is related to residual mass of polymer. The rest of mentioned ion

peaks (which do not belong to polymer distribution) may result from the formation of clusters, as combination of analyte, matrix and sodium ion.

Sample preparation procedure for characterization of Icon-Infiltrant was proposed. Optimal conditions were proposed as following, 40 mg DCTB /mL THF mixed with 5 mg NaTFA /mL THF resulting in 4.35:1 matrix-to-cationization reagent mixing ratio.

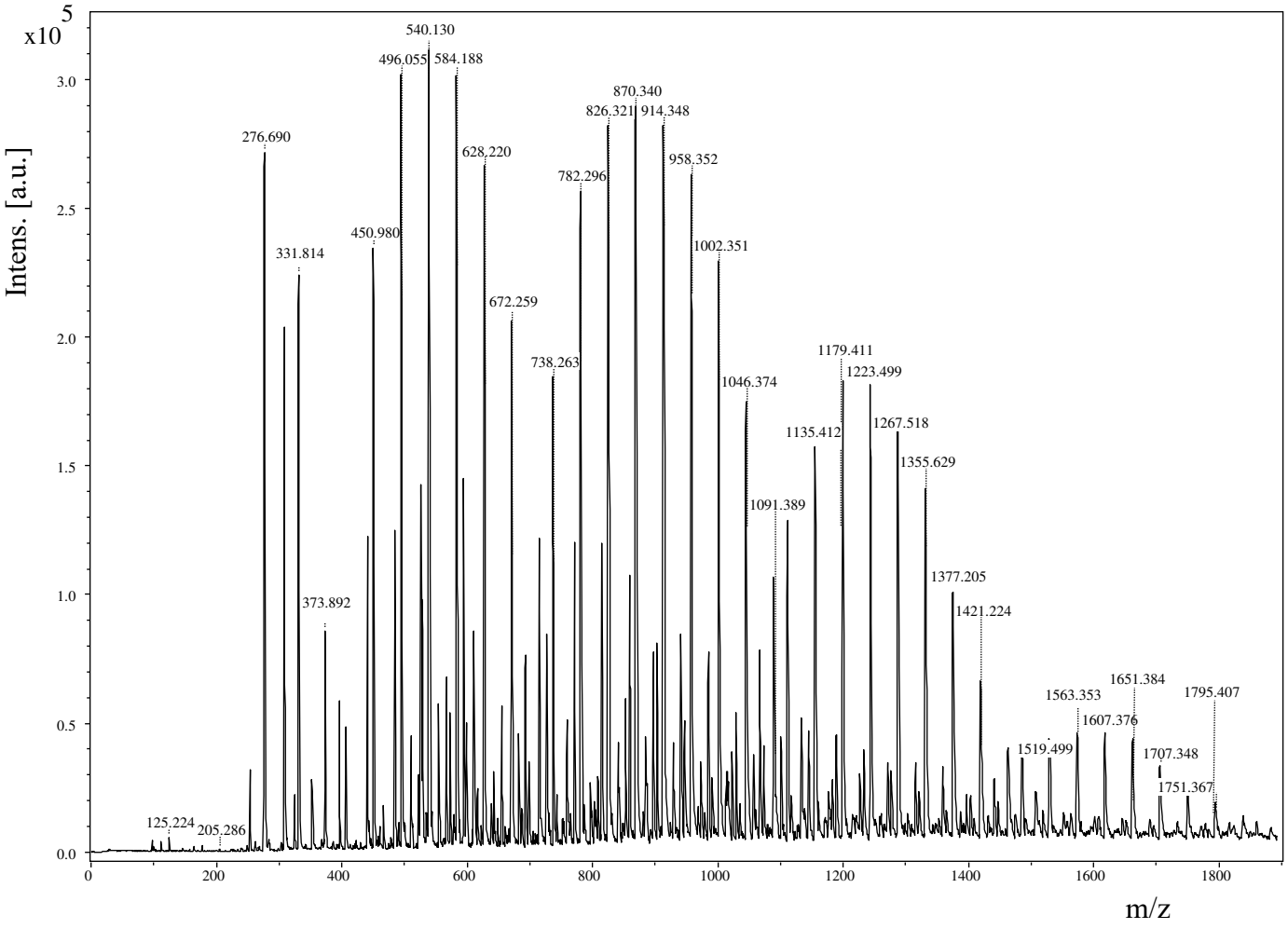

Figure 27 – MALDI MS spectrum of 0.8 µL Icon-Infiltrant covered with 0.8 µL matrix (40 mg DCTB/mL THF mixed with NaTFA cationization reagent 5 mg/mL at ratio of 4.35:1), accumulation of 1500 selected spectra, measured in linear mode.

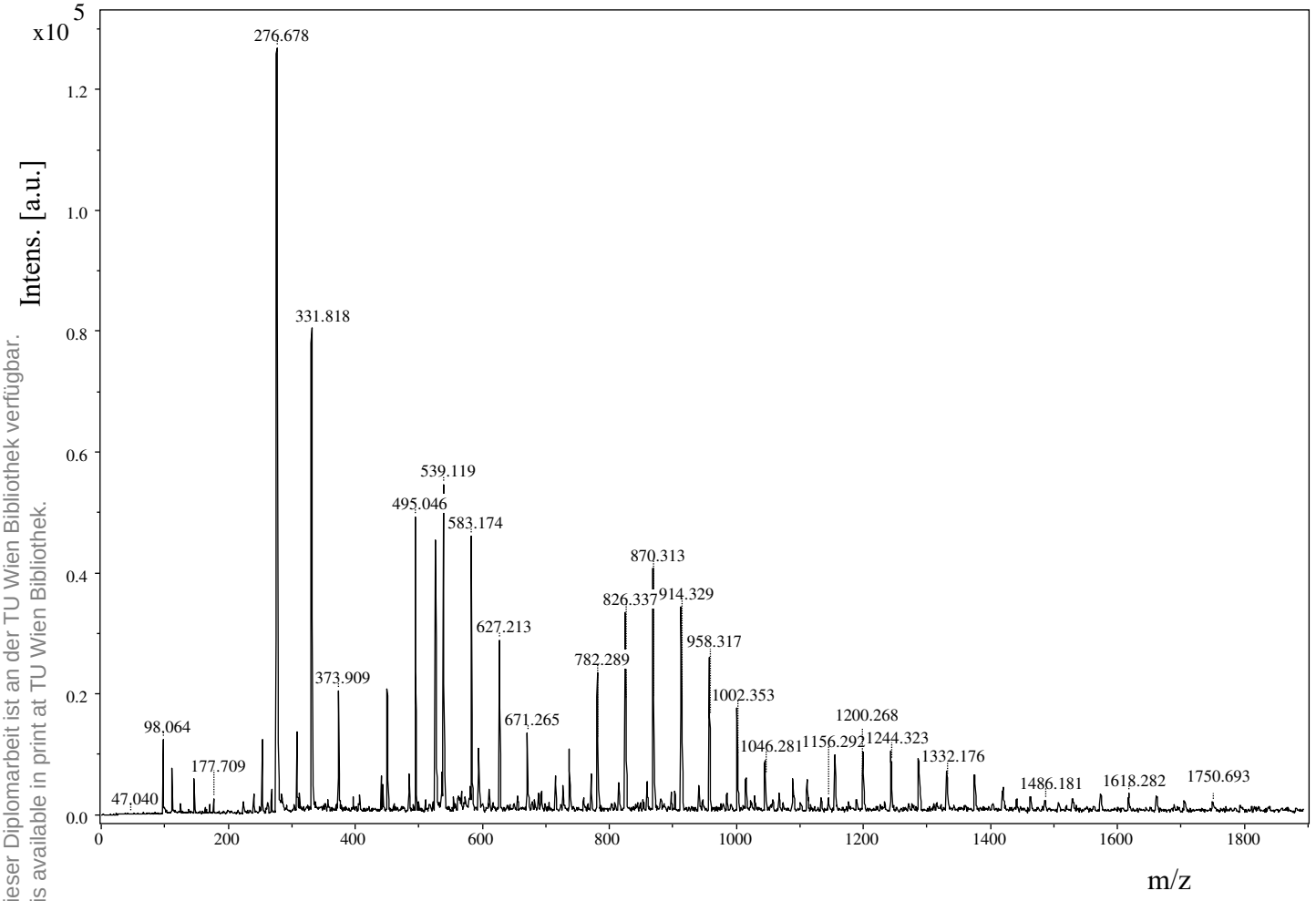

Figure 28 – MALDI MS spectrum of 0.8 µL Icon-Infiltrant covered with 0.8 µL matrix (40 mg DCTB/mL THF mixed with NaCl cationization reagent 5 mg/mL at ratio of 1.87:1), accumulation of 1500 selected spectra, measured in linear mode.

The $\Delta m/z$ of adjacent ion peaks might correspond to structure labelled with blue rectangle in Figure 29. Concentration in Icon-Infiltrant syringe content of Triethylene glycol dimethacrylate (TEDMA) is (70 – 95)% and concentration of Camphoro Quinone is < 2.5%. Therefore it can be assumed that distribution belongs to TEDMA and Camphoro Quinone was not detected.

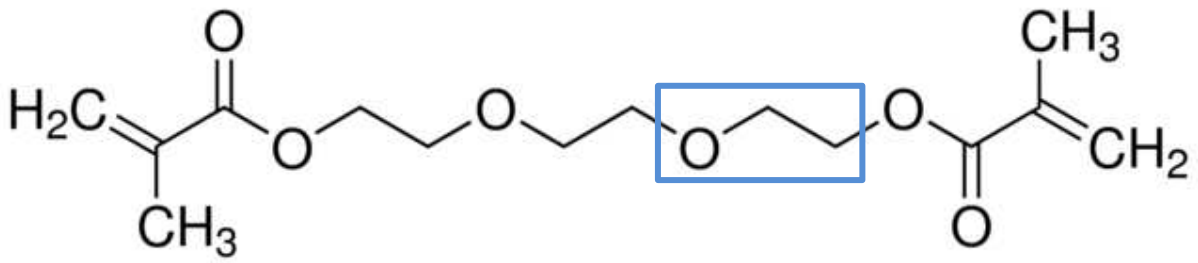

Figure 29 – Chemical structure of TEDMA. Part of structure labelled with blue rectangle corresponds to molecular weight 44 g/mol.

3.6 Human teeth sections

After characterization of Icon-Infiltrant by applying MALDI-TOF-MS was finished, further analyses with this dental material could be performed. The main purpose of this study was to measure Icon-Infiltrant on healthy human teeth sections. Therefore development of sample preparation protocol for cutting of human teeth was to be searched at first. Respectively, sample preparation procedure resulting in human teeth sections without embedding suitable for MALDI-TOF-MS analysis.

Process of cutting was carried out by using IsoMet™ Low Speed Saw (IsoMet 1000; Buehler; IsoMet 15HC, #11-4254, 0.3 mm, precision sectioning blade; Buehler). In this method, application of any glue was avoided and therefore no peaks related to glue can be expected in spectra. For that purpose, all human teeth were fixed to sample holder mechanically by clamping. When enamel structure of human tooth was reached during process of cutting, bending of applied blade was observed. Application of blades with high diamond concentration resulted in bending, thus, edge of majority human teeth sections had larger thickness value than the rest of human tooth section. This part was removed by scalpel and only part of acquired human tooth section with homogeneous thickness value was kept for further process. This value was measured by micrometer screw gauge and sections with thickness values suitable for target, used in measurement, were chosen only.

The first question was, if measurement of Icon-Infiltrant on obtained human teeth sections will be possible. Sample preparation procedure for this initial measurement involved the process of rinsing in turns, 2x in UHQ water and 2x in 2-Propanol. Clean human teeth sections were dried in ambient conditions and fixed to modified Waters target plate by electrically conductive double sided tape with conductive fibers (SHIMADZU, Korneuburg, Austria). Then, 10 µL DCTB matrix solution (40 mg/mL THF), 10 µL Icon-Infiltrant and 2.5 µL NaTFA cationization reagent solution (5 mg/mL

THF) were mixed. Afterwards, 0.8 µL of this mixture were applied directly on human teeth sections (100, 300 and 500 µm) by the pipette tip and dried in vacuum desiccator for 45 minutes. This solution was chosen according to results obtained in chapter 3.5, in which optimal conditions for characterization of Icon-Infiltrant were proposed. As expected, no spectra were obtained. Explanation for this outcome is missing electrical conductivity obligatory for instrument geometries.

Based on this outcome, three different sample preparation procedures were proposed for identification of Icon-Infiltrant on human teeth sections. Version 1 contains the same sample preparation procedure as described in previous paragraph with additional coating with gold. As it was already stated, the measurement resulted in no spectra due to missing electrical conductivity. Therefore coating with gold was proposed as first option that could be solution for achieving electrical conductivity and subsequent measurement of Icon-Infiltrant on human teeth sections. The aim of first measurement was to prove if coating with gold enables to measure Icon-Infiltrant on human teeth sections. Based on obtained results in version 1, version 2 and version 3 involved step of applying layer of gold.

3.6.1 Layer of gold as a solution for electrical conductivity (Version 1)

The objective of this measurement was to prove, if applied layer of gold will be adequate solution for obtaining spectra from measurement of Icon-Infiltrant on human teeth sections.

First, human teeth sections (200 and 300 µm) were coated with gold by using AGAR Gold-Sputter-Coater during the period 120 s and mixture with following parameters was prepared. Thus, 10 µL DCTB matrix solution (40 mg/mL THF), 10 µL Icon-Infiltrant and 2.5 µL NaTFA cationization reagent solution (5 mg/mL THF) were mixed. 0.8 µL of this mixture were applied directly on human teeth sections by the pipette tip and dried in vacuum desiccator for 45 minutes. Resulting spectra of this measurement can be seen in Figures 30 and 31. Applied layer of gold proved to be effective for obtaining data from measurements on human teeth sections. For that reason, this step was part of further measurements (Version 2 and 3) too. First settled value 120 seconds for coating with gold proved to be enough, therefore other time application periods were not tested.

Data obtained from human teeth sections, 2 polymer distributions in Figure 30 and 3 polymer distributions in Figure 31 can be seen. First two distributions of oligomers are in mass range 400-700 Da and 700-1100 Da, third in 1100-1400 Da.

For Figure 30, *m/z* values of most abundant peaks are 451.940 Da and 826.643 Da. Δ*m/z* of adjacent ion peaks can be expressed as Δ*m/z* 44.11 ± 0.04 Da for first distribution of oligomers and Δ*m/z* 44.08 ± 0.04 Da for second distribution of oligomers. The *m/z* values of most abundant peaks result in chain length 10 for first distribution of oligomers and 19 for second distribution of oligomers. Moreover, *m/z* 37.765 Da; *m/z* 67.787 Da; *m/z* 97.834 Da; *m/z* 146.990 Da; *m/z* 198.089 Da; *m/z* 236.058 Da; *m/z* 276.464 Da; *m/z* 325.824 Da; *m/z* 359.866 Da and *m/z* 368.680 Da were detected. Applied laser power was 50%.

For Figure 31, *m/z* values of most abundant peaks are 496.624 Da, 827.403 Da and 1202.047 Da. Δ*m/z* of adjacent ion peaks can be expressed as Δ*m/z* 44.12 ± 0.09 Da for first distribution of oligomers; Δ*m/z* 44.08 ± 0.01 Da for second distribution of oligomers and Δ*m/z* 44.21 ± 0.25 Da for third distribution of oligomers. Values of most abundant peaks result in chain length 11 for first distribution of oligomers; 19 for second distribution of oligomers and 27 for third distribution of oligomers. Furthermore, *m/z* 27.666 Da; *m/z* 54.104 Da; *m/z* 68.176 Da; *m/z* 98.038 Da; *m/z* 144.551 Da; *m/z* 198.421 Da; *m/z* 256.693 Da; *m/z* 276.892 Da; *m/z* 326.264 Da and *m/z* 361.656 Da were identified. Applied laser power was 56%.

After data obtained in this measurement were evaluated; comparison between spectra in Figures 30, 31 and spectrum in Figure 27 (chapter 3.5) could be done. In other words, difference between measurements of mixture proposed for characterization of Icon-Infiltrant on stainless-steel target (BRUKER Daltonics GmbH, Bremen, Germany) and on human teeth sections (200 and 300 µm) was to be observed. As it was already mentioned in chapter 3.5, *m/z* 276.690 Da in Figure 27 is assumed to belong to residual mass of polymer. The *m/z* 276.892 Da and *m/z* 276.464 Da were detected in Figures 30 and 31, which represent measurement of Icon-Infiltrant on human teeth sections (200 and 300 µm). Comparing most abundant *m/z* peaks, lower values were detected in spectra from measurement on human teeth sections. Δ*m/z* varied only in decimals. Values of *m/z* 67.787 Da; *m/z* 97.834 Da; *m/z* 198.089 Da and *m/z* 325.824 Da were identified in Figure 30. Values of *m/z* 68.176 Da; *m/z* 98.038 Da; *m/z* 198.421 Da and *m/z* 326.264 Da were identified in Figure 31. These values were not identified in Figure 27. To find out if these values belong to human teeth, more measurements must be performed.

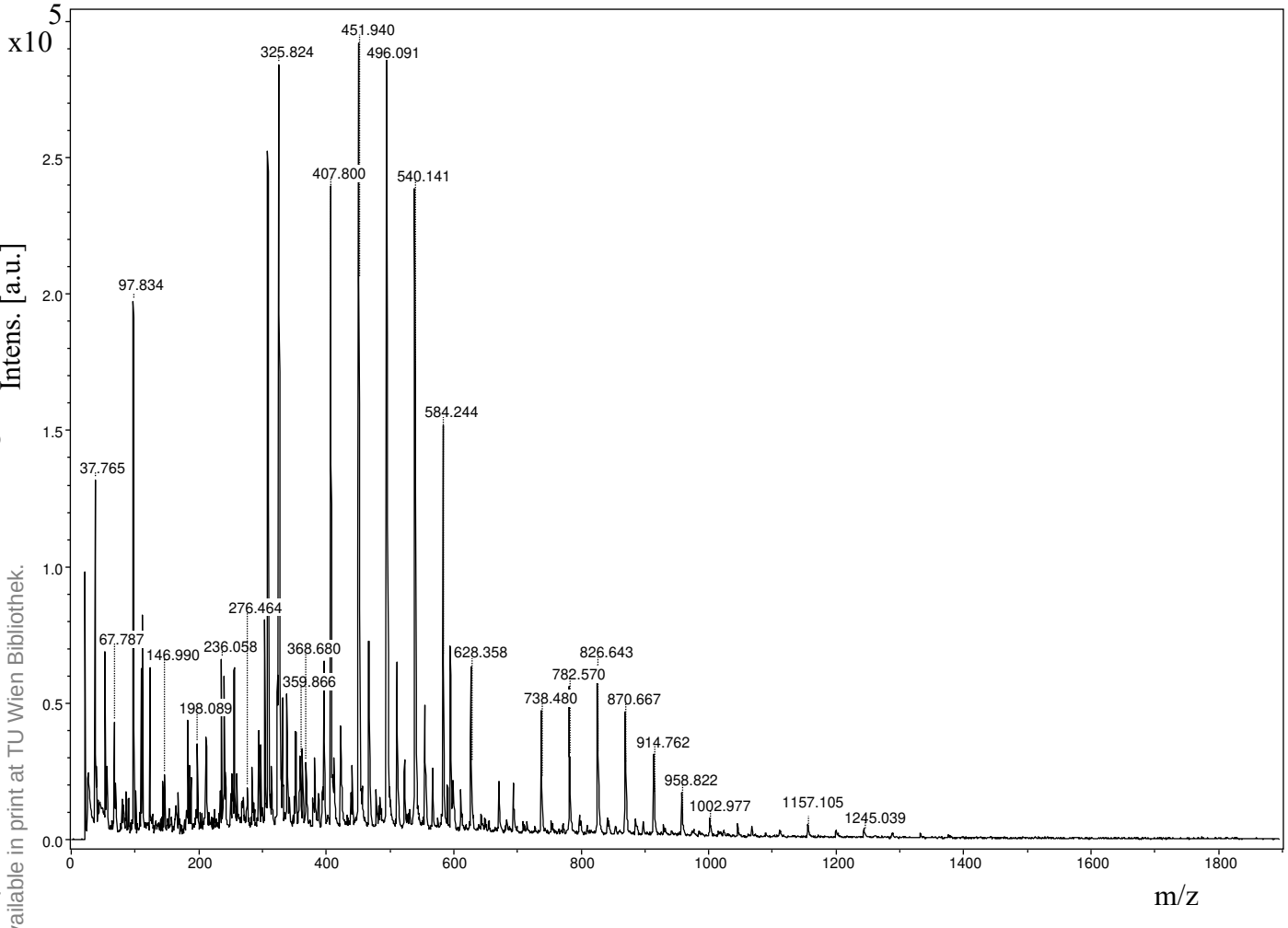

Figure 30 – MALDI MS spectrum of 0.8 µL mixture (40 mg DCTB/mL THF mixed with NaTFA cationization reagent 5 mg/mL THF at ratio of 4.35:1 and Icon-Infiltrant; DCTB:Icon-Infiltrant:NaTFA were mixed in 4:4:1, v/v/v) measured on human tooth section (thickness: 200 µm) covered with gold, accumulation of 1600 selected spectra, measured in linear mode.

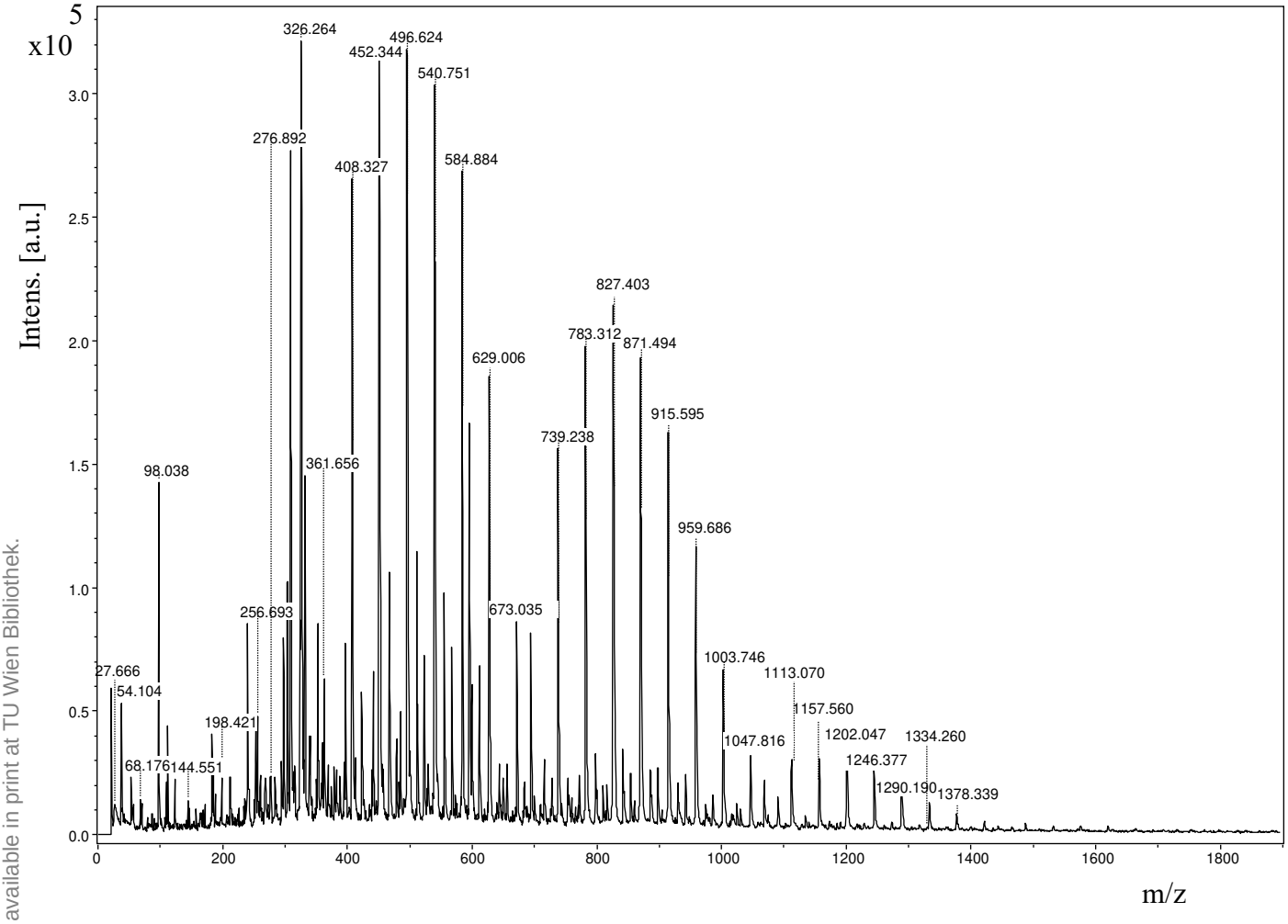

Figure 31 – MALDI MS spectrum of 0.8 µL mixture (40 mg DCTB/mL THF mixed with NaTFA cationization reagent 5 mg/mL THF at ratio of 4.35:1 and Icon-Infiltrant; DCTB:Icon-Infiltrant:NaTFA were mixed in 4:4:1, v/v/v) measured on human tooth section (thickness: 300 µm) covered with gold, accumulation of 1300 selected spectra, measured in linear mode.

3.6.2 Matrix sublimation and MS Imaging (Version 2)

As applied layer of gold on human teeth sections proved to be solution for obtaining spectra, this step was performed as part of sample preparation procedure in this measurement too.

Determination and visualization of sublimed DCTB matrix and Icon-Infiltrant on human teeth sections by MS Imaging were aim of this measurement. The sublimation technique for matrix application has several notable features. The enhanced purity of matrix applied to the sample, the very small crystal size, and uniformity of deposition are factors that contribute to images with high definition [62]. For that reason, performance of this matrix application technique in this study was matter of interest.

2 forms of human teeth sections (200 and 500 µm) were analysed. In first form, Icon-Infiltrant was not applied and human teeth sections were covered with gold. In second form, 0.8 µL Icon-Infiltrant were applied on human teeth sections by the pipette tip and dried in vacuum desiccator for 45 minutes. Afterwards, coating with gold was performed.

As it was already mentioned in 2.2.7.2, the home-built sublimation device was used to sublime matrix. 25 mg of DCTB matrix per 3.8 mL Acetone/Acetonitrile (7:3; v/v) were placed in a preheated well (63 °C) forming a homogeneous microcrystalline matrix layer after solvent evaporation. Based on studies of the variation in deposited DCTB layers with sublimation parameters [63], sublimation of this matrix was done at 80 ºC. Temperature resulted in homogeneous coverage of this matrix, therefore further temperature variations in matrix sublimation were not examined. Sublimation was preceded until matrix crystals in the well volatilized entirely (10 min). Sublimation of 25 mg per DCTB matrix resulted in a coating of 0.15 mg/cm².

Microscope images of sublimed DCTB matrix can be seen in Figure 33. Spectra obtained in measurement of DCTB matrix on modified Waters target plate and on gold-covered human tooth section of thickness 200 µm (without applied Icon-Infiltrant) were compared with mMass software (Figure 32). Spectra obtained in this measurement can be seen in Figures 34 – 36. Image obtained in MS Imaging can be seen in Figure 37.

For Figure 34, *m/z* values of most abundant peaks are 495.388 Da, 825.735 Da and 1200.122 Da. $\Delta m/z$ of adjacent ion peaks can be expressed as $\Delta m/z$ 44.05 ± 0.01 Da for first distribution of oligomers; $\Delta m/z$ 44.05 ± 0.03 Da for second distribution of oligomers and $\Delta m/z$ 44.05 ± 0.01 Da for third distribution of oligomers. Values of most abundant peaks result in chain length 11 for first

distribution of oligomers; 19 for second distribution of oligomers and 27 for third distribution of oligomers. Furthermore, *m/z* 39.154 Da; *m/z* 99.16 Da; *m/z* 137.121 Da; *m/z* 195.187 Da; *m/z* 235.220 Da; *m/z* 277.307 Da; *m/z* 309.247 Da and *m/z* 326.498 Da were identified.

For Figure 36, *m/z* values of most abundant peaks are 495.517 Da, 825.943 Da and 1200.389 Da. Δ*m/z* of adjacent ion peaks can be expressed as Δ*m/z* 44.06 ± 0.01 Da for first distribution of oligomers; Δ*m/z* 44.06 ± 0.02 Da for second distribution of oligomers and Δ*m/z* 44.06 ± 0.01 Da for third distribution of oligomers. Values of most abundant peaks result in chain length 11 for first distribution of oligomers; 19 for second distribution of oligomers and 27 for third distribution of oligomers. Furthermore, *m/z* 39.164 Da; *m/z* 69.188 Da; *m/z* 99.184 Da; *m/z* 148.198 Da; *m/z* 195.218 Da; *m/z* 235.253 Da; *m/z* 304.486 Da; *m/z* 309.309 Da; *m/z* 356.595 Da; and *m/z* 391.427 Da were identified.

What else could be observed, higher intensity of peak *m/z* 697.554 Da in Figure 34 and of peak 697.715 in Figure 36 was identified. This value was not used in calculation of Δ*m/z*. Comparing values of applied laser power, spectrum in Figure 35 was obtained with laser power 34%. Laser power required to obtain spectra in Figures 34 and 36 was 85%, since energy required for desorption and ionisation of analyte co-crystallized with matrix is higher.

Comparing spectra obtained in measurement (chapter 3.6.2) of sublimed DCTB matrix on human tooth section covered with gold (500 µm) in Figure 35 and of sublimed matrix on human tooth section covered with gold (500 µm) and containing Icon-Infiltrant in Figure 36, following *m/z* values were observed. The *m/z* values 195.206 Da, 235.240 Da, 356.600 Da, 392.440 Da, 1002.301 Da and 1156.510 Da were detected in Figure 35; 195.218 Da, 235.253 Da, 356.595 Da, 391.427 Da, 1002.194 Da and 1156.325 Da were detected in Figure 36. These peaks may result from the formation of clusters, as combination of DCTB matrix and mineral ions present in human teeth.

Following *m/z* values were identified only in spectra of this measurement, where measurement was performed on human teeth sections. Thus, these peaks were not observed in Figure 35, which represents measurement on modified Waters target plate. Figure 34, *m/z* values 39.154 Da, 99.16 Da, 309.247 Da and *m/z* values 39.164 Da, 99.184 Da and 309.309 Da in Figure 36. Since these ion peaks were not detected in measurements discussed in chapters 3.6.1 and 3.6.3, it can not be clearly stated that these ion peaks come from human teeth. Further measurements must be performed to elucidate these peaks.

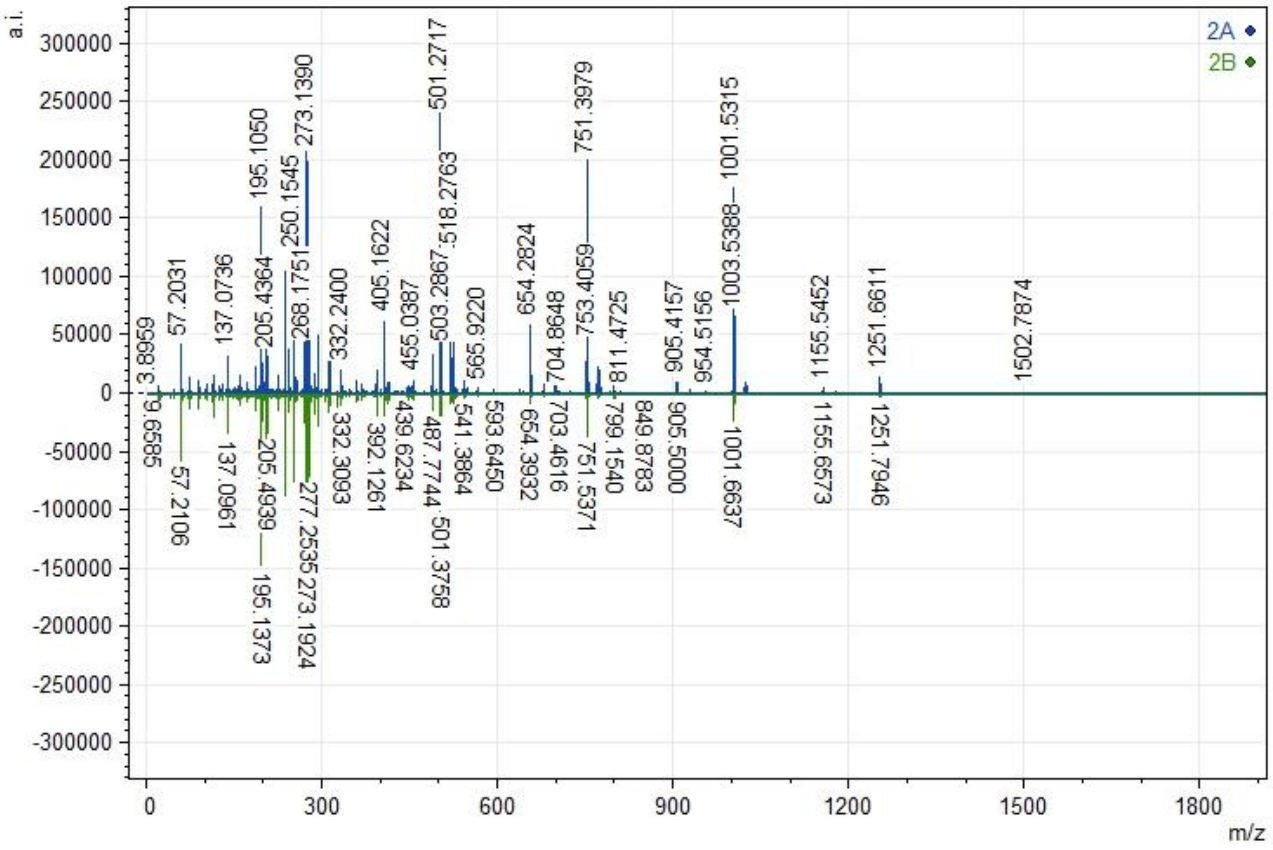

Figure 32 – Blue - MALDI MS spectrum of sublimed DCTB matrix measured on modified Waters target plate, accumulation of 1300 selected spectra, measured in reflectron mode. Green - MALDI MS spectrum of sublimed DCTB matrix measured on human tooth section (thickness: 200 µm) covered with gold, accumulation of 1600 selected spectra, measured in reflectron mode.

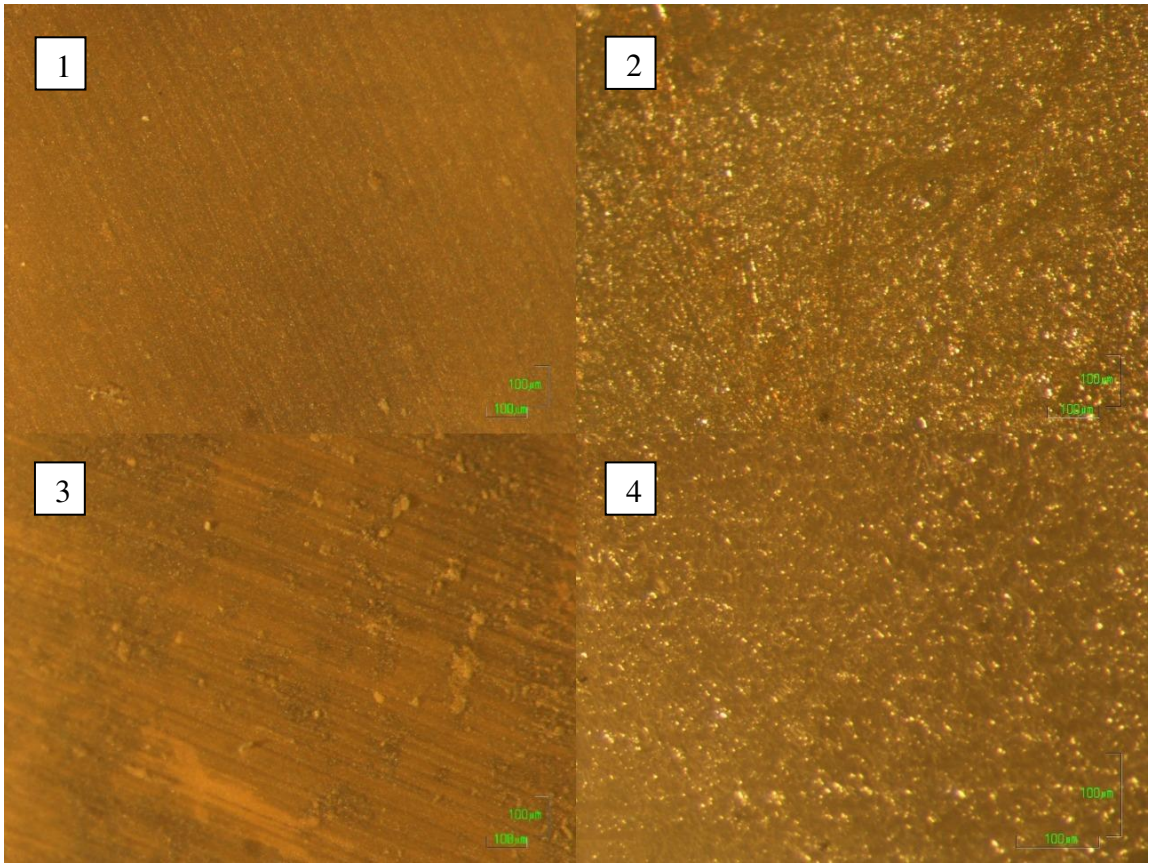

Figure 33 – (1): Distribution of sublimed DCTB matrix on human tooth section (thickness: 200 µm); (2) Distribution of sublimed DCTB matrix on human tooth section (thickness: 200 µm) with applied Icon-Infiltrant; (3) Distribution of sublimed DCTB matrix on human tooth section (thickness: 500 µm); (4) Distribution of sublimed DCTB matrix on human tooth section (thickness: 500 µm) with applied Icon-Infiltrant.

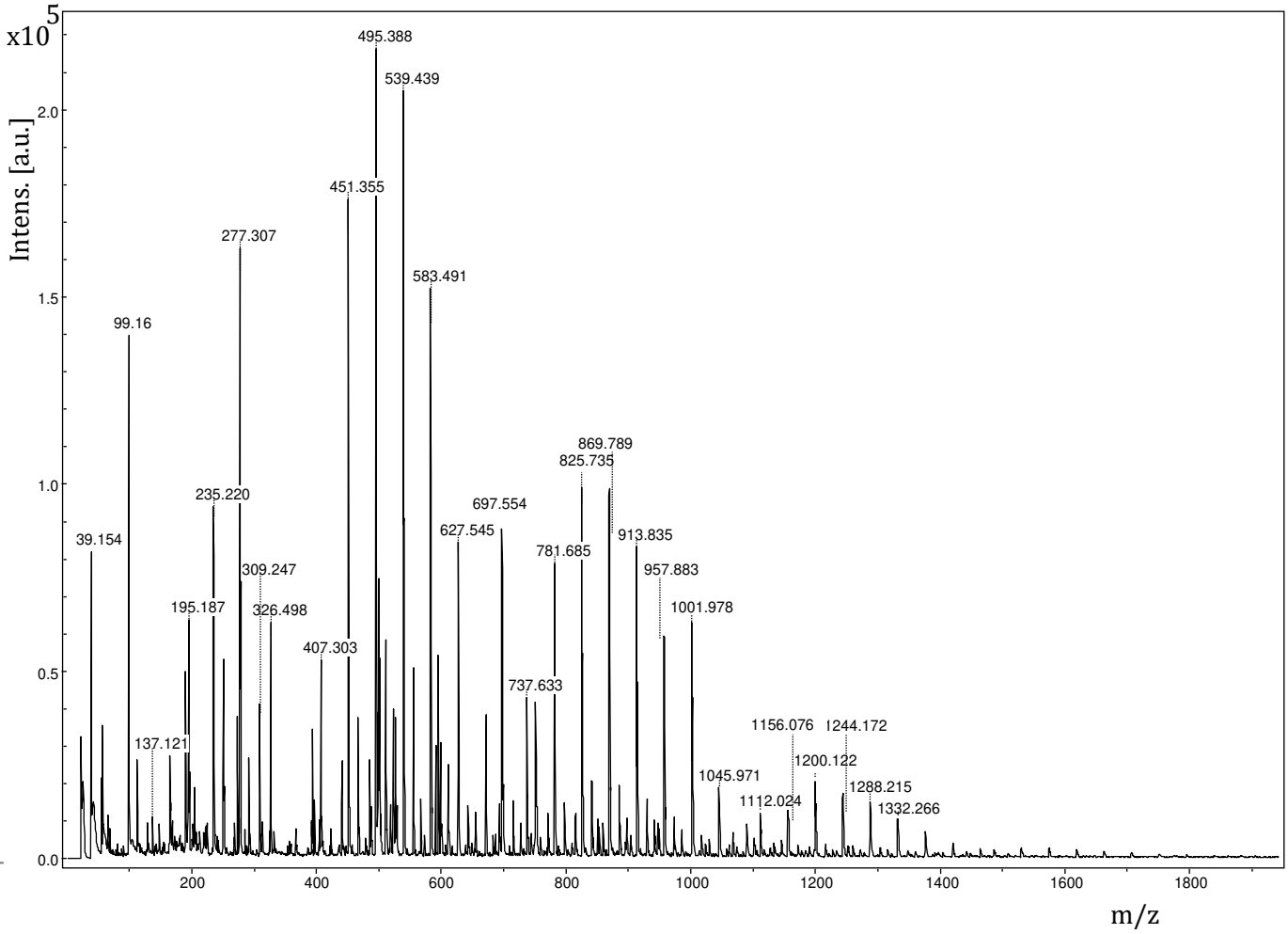

Figure 34 – MALDI MS spectrum of sublimed DCTB matrix measured on human tooth section (thickness: 200 µm) covered with gold and 0.8 µL Icon-Infiltrant, accumulation of 1700 selected spectra, measured in reflectron mode.

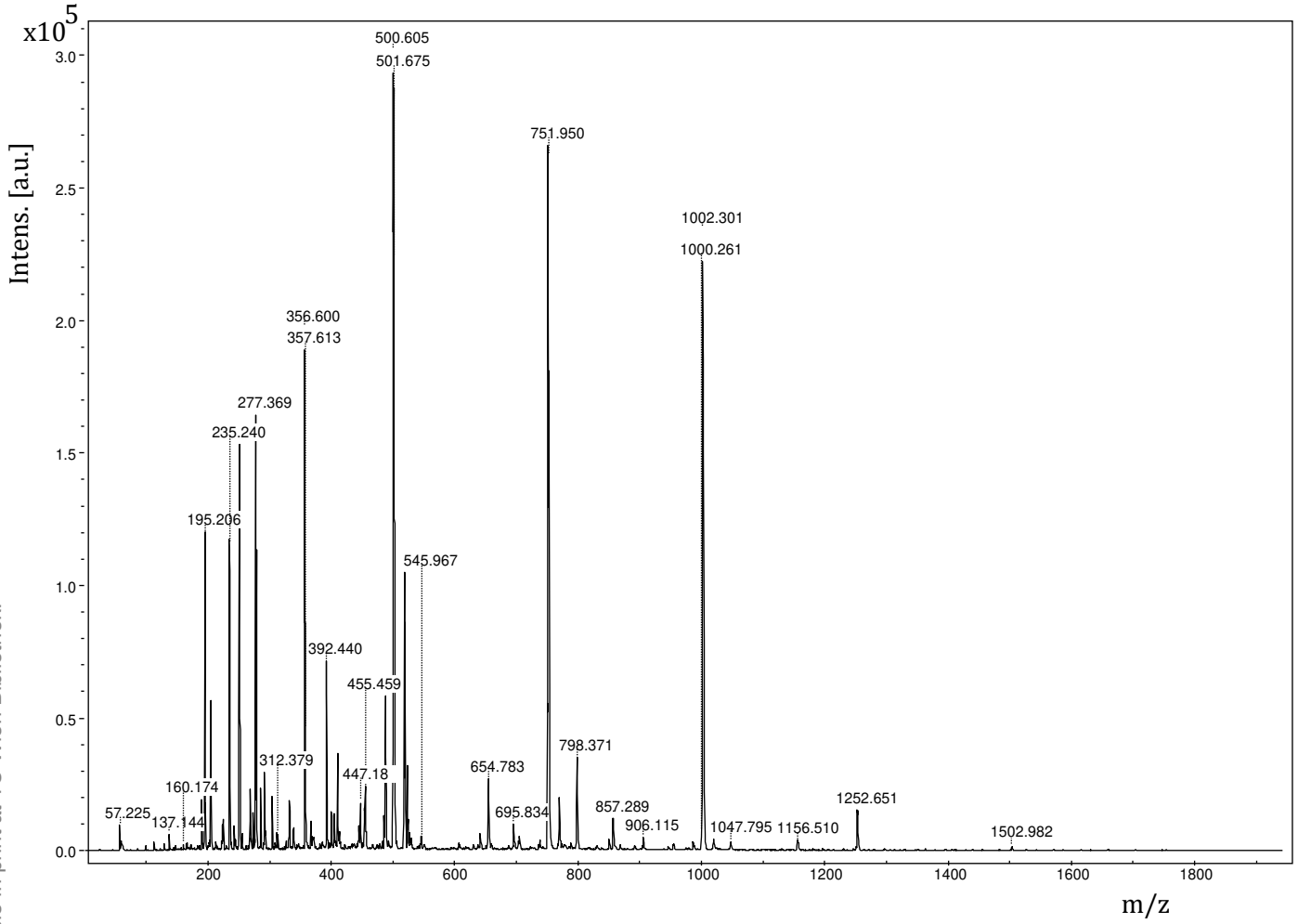

Figure 35 – MALDI MS spectrum of sublimed DCTB matrix measured on human tooth section (thickness: 500 µm) covered with gold, accumulation of 1600 selected spectra, measured in reflectron mode.

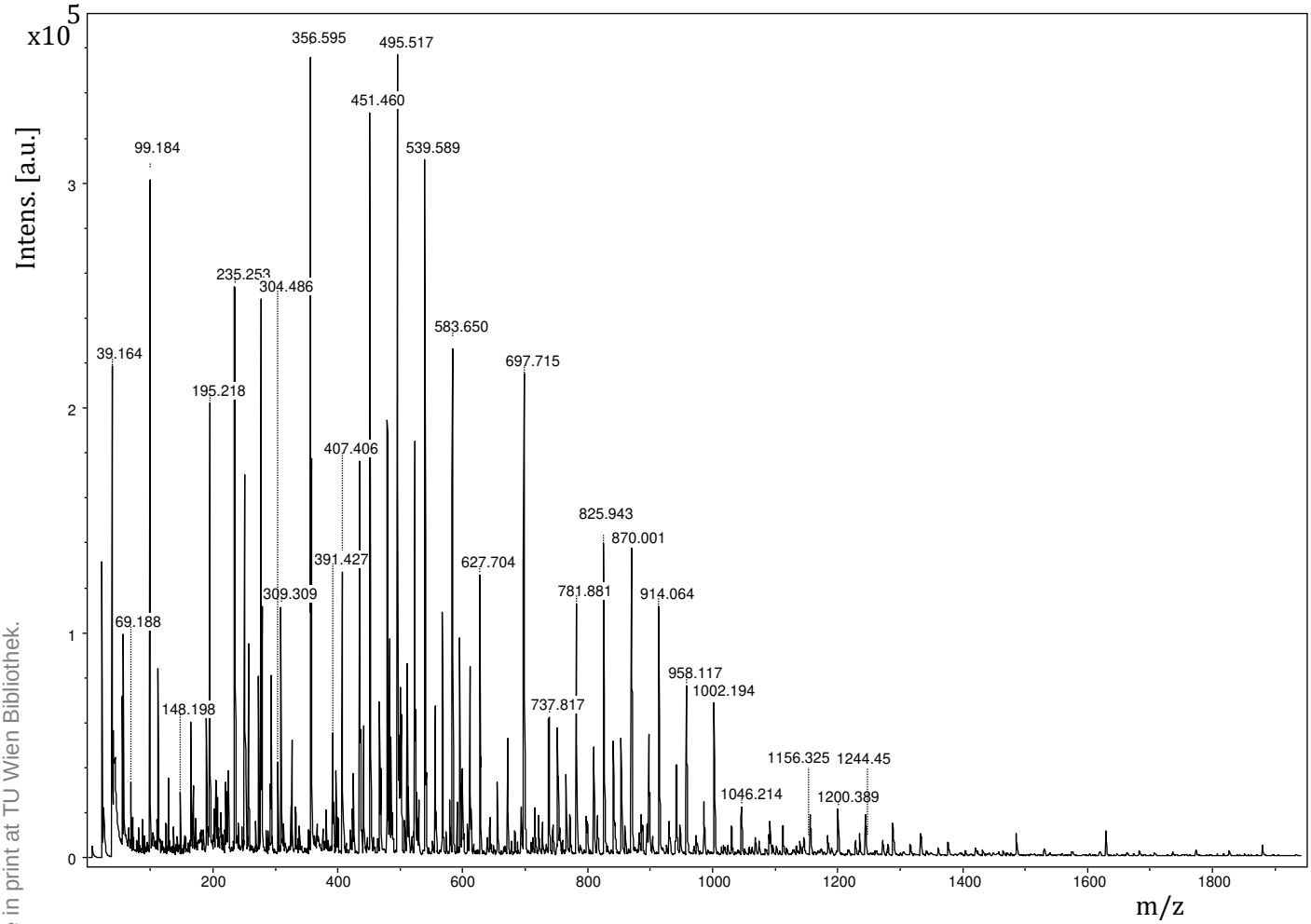

Figure 36 – MALDI MS spectrum of sublimed DCTB matrix measured on human tooth section (thickness: 500 µm) covered with gold and 0.8 µL Icon-Infiltrant, accumulation of 1800 selected spectra, measured in reflectron mode.

Figure 37 – Results obtained in MSI expriment. Coloured regions correspond to following *m/z* values: Red (250.34 Da) - DCTB matrix; Green (540.13 Da ± 0.5 Da), Blue (870.34 Da ± 0.5 Da), Yellow (1179.41 Da ± 0.5 Da), Purple (1563.35 Da ± 0.5 Da) - Icon Infiltrant; 1) Left – sublimed DCTB matrix on human tooth section (thickness: 200 µm) covered with gold; right – sublimed DCTB matrix on human tooth section (thickness: 200 µm) covered with gold and 0.8 µL Icon-Infiltrant; 2) sublimed DCTB matrix on human tooth section (thickness: 500 µm) covered with gold; right – sublimed DCTB matrix on human tooth section (thickness: 500 µm) covered with gold and 0.8 µL Icon-Infiltrant; 3) Sublimed DCTB matrix on modified Waters target plate.

3.6.3 Icon-Infiltrant under layer of gold and droplet of matrix on the top (Version 3)

In this sample preparation procedure, 0.8 µL Icon-Infiltrant were applied on human teeth sections (200 and 700 µm) as first. Afterwards, coating with gold was performed. Droplet of 40 mg DCTB /mL solution was applied on human tooth sections covered with gold. In comparison to Version 1, Icon-Infiltrant was applied before covering with gold and no cationization reagent was applied in this measurement.

Result of this measurement can be seen in Figure 38. This spectrum was obtained with laser power 42%. 3 distrubutions of oligomers in mass ranges 100-400 Da, 400-700 Da and 700-1000 Da can be observed. For Figure 38, *m/z* values of most abundant peaks are 270.363 Da, 492.860 Da and

825.288 Da. Δ*m/z* was not calculated for first polymer distribution. Δm/z could not be correctly calculated due to presence of other peaks. Moreover, the *m/z* 34.33 Da; *m/z* 50.45 Da; *m/z* 81.80 Da and *m/z* 97.19 Da were identified in mass range 0-100 Da. Δ*m/z* of adjacent ion peaks can be expressed as Δ*m/z* 44.35 ± 0.49 Da for second distribution of oligomers and Δ*m/z* 44.17 ± 0.03 Da for third distribution of oligomers. Values of most abundant peaks result in chain length 11 for second distribution of oligomers and 19 for third distribution of oligomers. What else could be observed in Figures 38, higher intensity for peak *m/z* 696.62 Da was identified. This value was not used in calculation of Δ*m/z*.

As it was already mentioned, no cationization reagent was used in this measurement. Explanation for obtaining polymer distributions can be fact that human teeth contain large amount of minerals including sodium and this resulted in ionisation of analyte.

Now, comparison of *m/z* values between spectra obtained from measurements on human teeth sections can be done.

Certain shifts between *m/z* values in all spectra obtained on human teeth sections may result from inhomogenous surface. Even though homogenous surface of human teeth sections were to be obtained, small-sized embeddings may occur. These can result from manipulation by tweezers during cleaning or from removing of edge with higher thickness by scalpel.

High intensities of ion signals were obtained from measurements on human teeth sections. Since measurement of Icon-Infiltrant on stainless-steel target (BRUKER Daltonics GmbH, Bremen, Germany) is achieved only by application of cationization reagent, present mineral ions in human teeth are supporting ionisation process of polymer in Icon-Infiltrant on human teeth sections. This statement is supporting result obtained in Figure 38, where distributions of oligomers were obtained, even though no cationization reagent was applied in sample preparation procedure.

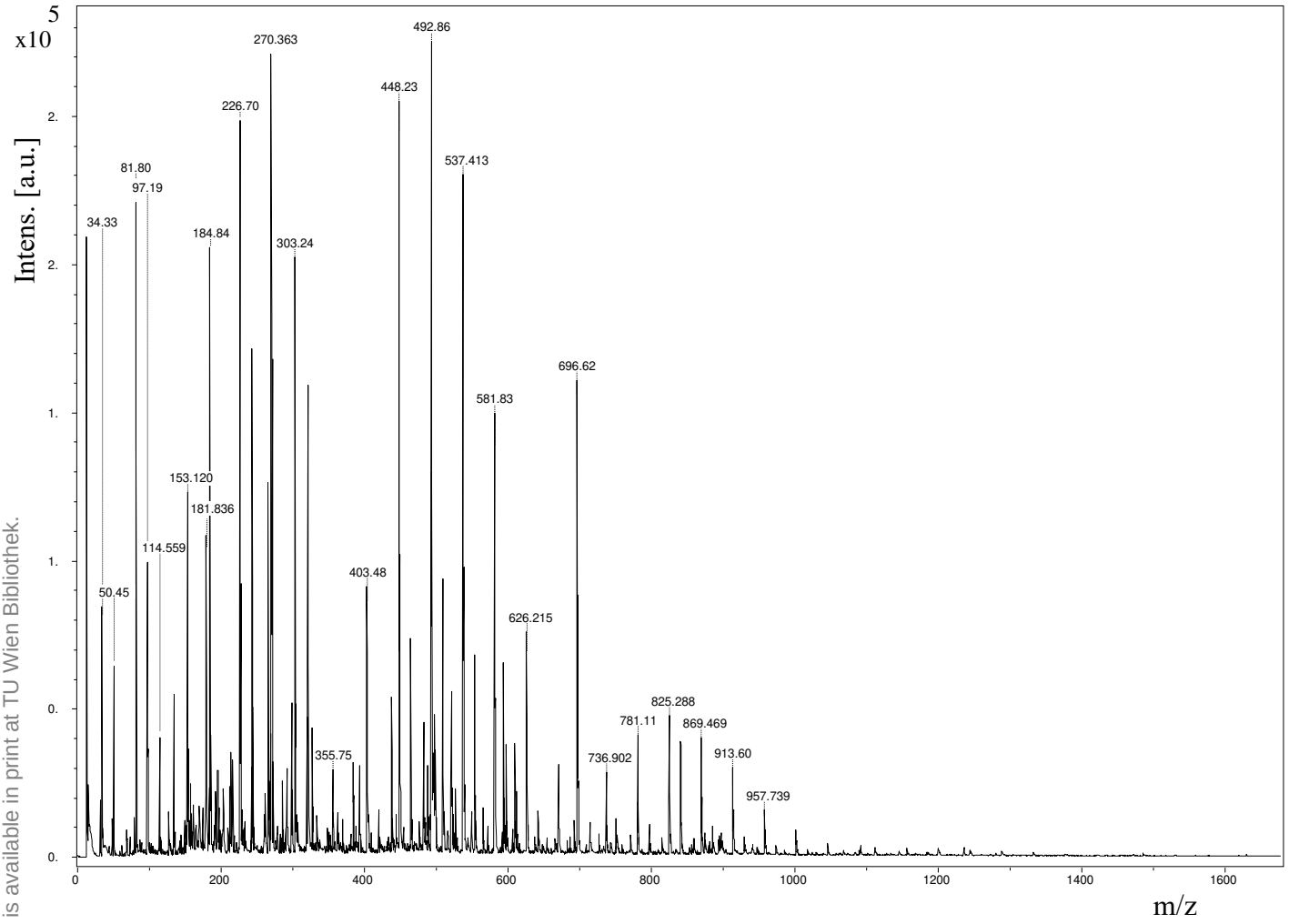

Figure 38 – MALDI MS spectrum of 0.8 µL solution (40 mg DCTB/mL THF) measured on human tooth section (thickness: 700 µm) covered with 0.8 µL Icon-Infiltrant and gold, accumulation of 1200 selected spectra, measured in reflectron mode.

4. Conclusion

It is well known that MALDI-TOF-MS is a sensitive and versatile analytical technique for detecting and characterizing a wide variety of compounds. The MSI community is continuously improving its sample preparation processes to produce more robust protocols and to get most of the tissues analysed. Based on promising results obtained from first analysis on human teeth with MALDI-TOF-MSI by Hirano and co-workers [1], further application of this analytical technique on human teeth samples is matter of interest. Present thesis serves as a proof-of-principle study for reaching the ultimate goal of an *in vitro* study, which aims at the examination of proximal natural incipient

carious lesions after resin infiltration (Icon; DMG) to get a deeper understanding of the spatial distribution of the resinous caries infiltrant and to identify yet unknown organic molecules by MALDI MS and MSI.

The first outcome of this study, was the characterization of product "*DMG Icon® – Caries infiltrant – proximal*". Icon-Dry and Icon-Infiltrant syringe contents showed both polymer distributions although Icon-Dry was not expected to contain any polymer. Yet, both samples were used to develop a proper sample preparation strategy and to find optimal measurement conditions in order to obtain meaningful mass spectra. Presence of polymer component in Icon-Dry syringe can not be clearly explained as this sample was described to contain only ethanol. A tentative explanation is leaching of polymers from the plastic syringe holding the alcohol solution. Sample preparation was developed using Dithranol as matrix. However, Dithranol production with a purity ≥ 98.0% was discontinued by the vendor and therefore an alternative matrix had to be found. THAP was found to be useful and the final sample preparation for Icon-Dry was as follows: 10 mg THAP/mL and 2 mg AgTFA/mL (5:1 matrix-to-cationization reagent mixing ratio) were weighted in eppendorf tube and dissolved in THF. 0.8 µL Icon-Dry and 0.8 µL mixture (comprising matrix and cationization reagent) were applied by the pipette tip on stainless-steel targets (BRUKER Daltonics GmbH, Bremen, Germany). Each volume application was followed by drying in ambient conditions.

Same considerations were taken into account when the optimized sample preparation protocol for Icon-Infiltrant was developed. Procedure for finding the optimal conditions included variation of parameters such as matrix, cationization reagent, matrix-to-cationization reagent mixing ratio and solvents. The optimal sample preparation for Icon-Infiltrant was as follows: Solutions of 40 mg DCTB/mL THF and 5 mg NaTFA/mL THF resulting in 4.35:1 matrix-to-cationization reagent mixing ratio were prepared. Dried-droplet method was applied. Thus, 10 µL matrix solution, 10 µL Icon-Infiltrant and 2.5 µL cationization reagent solution were mixed in eppendorf tube. Afterwards, 0.8 µL were applied directly on stainless-steel target (BRUKER Daltonics GmbH, Bremen, Germany) by the pipette tip and dried in vacuum desiccator for 45 minutes.

It was found that the polymer distribution observed in Icon-Dry was not the same as for Icon-Infiltrant allowing therefore a differentiation of the two components even in mixtures, which is of importance for future experiments.

The second part of this thesis was focused on MALDI-TOF-MS measurement of Icon-Infiltrant applied on healthy human teeth sections. Based on the characterization of Icon-Infiltrant carried out in the first part of this thesis, mass spectra gathered from teeth were compared to the mass spectra

of the plain polymer solution. As a pre-requisit for this task teeth samples had to be cut in µm-thick sections. However, as it was already mentioned above, the mechanical properties of human teeth are determined by their structure and composition and it is important to point out the fact that enamel is the most mineralized tissue of human body and its hardness is based primarily on inorganic material, the hydroxyapatite ($Ca_5(PO_4)_3(OH)$). Based on this knowledge, proper cutting procedures had to be proposed. Human teeth were mechanically fixed to a sample holder by clamping and the application of any type of glue was avoided. Using a diamond blade (IsoMet 15HC, #11-4254, 0.3 mm) the teeth were cut into 100 to 700 µm thin tissue sections. Interestingly, when the enamel structure of the human tooth was reached while cutting, bending of the blade was observed. For future work lower diamond concentration in the blade are suggested as higher forces are applied by each single crystal and cutting can be performed with reduced bending of the blade. Application of blades with high diamond concentration resulted in bending, thus, the edges of the majority of the teeth sections were thicker than the rest of the section. This part was removed by a scalpel and only the part with a homogeneous thickness was kept for further processing. This value was measured by micrometer screw gauge and sections of appropriate thickness were used in further experiments.

The inorganic composition of the teeth had not implications for the cutting process but also affected MALDI TOF MS experiments. Hydroxyapatite is an insulating material hindering an efficient desorption/ionisation process when a voltage of 20kV shall be applied to the sample holder. Coating of the teeth sections with a gold layer proved to be effective for obtaining reasonable data from MALDI experiments. Sputtering gold for 120 seconds provided good coating of the sample and no other time setting was tested. All further human teeth sections were measured after gold sputtering.

Measurement on human teeth sections of different thickness was successfully performed and the presence of Icon-Infiltrant detectable using different sample preparation protocols.

Interestingly, even though the detection of expected polymer chains was possible (polymer distribution), signal intensity levels changed when comparing mass spectra of the plain polymer and mass spectra generated from teeth surfaces. An explanation for difference in these values can be a matter of further discussion and more research would be required to obtain clear explanation.

5. References

1. Hirano, H., et al., *Matrix-assisted laser desorption/ionization imaging mass spectrometry revealed traces of dental problem associated with dental structure.* Anal Bioanal Chem, 2014. **406**(5): p. 1355-63.
2. Microbeonline. *MALDI-TOF Mass Spectrometry: Principle and Applications in Microbiology [Internet]*. [cited 2019 May 23]; Available from: https://microbeonline.com/maldi-tof-ms-principle-applications-microbiology/.
3. Porta Siegel, T., et al., *Mass Spectrometry Imaging and Integration with Other Imaging Modalities for Greater Molecular Understanding of Biological Tissues.* Mol Imaging Biol, 2018. **20**(6): p. 888-901.
4. Ono, M., et al., *Practical whole-tooth restoration utilizing autologous bioengineered tooth germ transplantation in a postnatal canine model.* Sci Rep, 2017. **7**: p. 44522.
5. Yamamoto, T., et al., *Histology of human cementum: Its structure, function, and development.* The Japanese dental science review, 2016. **52**(3): p. 63-74.
6. Medical News. *What is Dentin / Dentine?* [cited 2019 May 15]; Available from: https://www.news-medical.net/health/What-is-Dentin-Dentine.aspx.
7. Goldberg, M., *Understanding Dental Caries From Pathogenesis to Prevention and Therapy*. 2016.
8. Fujita, T., et al., *Regulation of defensive function on gingival epithelial cells can prevent periodontal disease.* The Japanese dental science review, 2018. **54**(2): p. 66-75.
9. Barczyk, M., A.I. Bolstad, and D. Gullberg, *Role of integrins in the periodontal ligament: organizers and facilitators.* Periodontology 2000, 2013. **63**(1): p. 29-47.
10. Dictionary by Merriam-Webster. *Definition of mass spectrometry [Internet]*. [cited 2019 Mar 3]; Available from: https://www.merriam-webster.com/dictionary/mass%20spectrometry.
11. Gross, J.H., *Mass Spectrometry : A Textbook.* 2011.
12. PREMIER Biosoft @ASMS 2018. *References, Mass Spectrometry [Internet]*. [cited 2019 May 20]; Available from: http://www.premierbiosoft.com/tech_notes/mass-spectrometry.html.
13. Medhe, S., *Ionization Techniques in Mass Spectrometry: A Review*. Vol. 4. 2018.

14. Lottspeich, F., J.W. Engels, and V.C.H. Wiley, *Bioanalytics : analytical methods and concepts in biochemistry and molecular biology*. 2018.
15. De Hoffmann, E. and V. Stroobant, *Mass spectrometry : principles and applications*. 2012, Chichester [etc.]: John Wiley.
16. Ho, C.S., et al., *Electrospray ionisation mass spectrometry: principles and clinical applications.* The Clinical biochemist. Reviews, 2003. **24**(1): p. 3-12.
17. MALDI - Matrix-Assisted Laser Desorption/Ionization | Biomolecular Analysis Facility. [cited 2019 May 15]; Available from: https://med.virginia.edu/biomolecular-analysis-facility/equipment/maldi-matrix-assisted-laser-desorptionionization/.
18. Creative Proteomics. *MALDI-TOF Mass Spectrometry [Internet]*. [cited 2019 Mar 5]; Available from: https://www.creative-proteomics.com/technology/maldi-tof-mass-spectrometry.htm.
19. Setou, M., *Imaging mass spectrometry protocols for mass microscopy.* 2010.
20. Holzlechner, M., *MALDI mass spectrometric imaging - aspects of sample preparation*. 2018, Technische Universität Wien.
21. Sigma-Aldrich. *Matrix Substances for MALDI-MS [Internet]*. [cited 2019 Mar 4]; Available from: https://www.sigmaaldrich.com/analytical-chromatography/analytical-products.html?TablePage=103431784.
22. Gessel, M.M., J.L. Norris, and R.M. Caprioli, *MALDI imaging mass spectrometry: spatial molecular analysis to enable a new age of discovery.* Journal of proteomics, 2014. **107**: p. 71-82.
23. Cascade Dental: Dentist Vancouver WA | Family and Cosmetic Dentistry. [cited 2019 May 15]; Available from: https://cascadesdental.com/ct-scans-in-dentistry/.
24. Dental X-Rays - UCSB Student Health - UC Santa Barbara. [cited 2019 May 15]; Available from: http://studenthealth.sa.ucsb.edu/medical-services/dental-care/dental-x-rays.
25. Dictionary by Merriam-Webster: America's most-trusted online dictionary. [cited 2019 May 2]; Available from: https://www.merriam-webster.com/medical/gumline.
26. Able Dental Group. *Diagnostic Equipment and Procedures [Internet]*. [cited 2019 Mar 2]; Available from: https://www.abledentalgroup.com/services/diagnostic.
27. Oral health - World Health Organization. [cited 2019 May 15]; Available from: https://www.who.int/news-room/fact-sheets/detail/oral-health.

28. Forssten, S.D., M. Björklund, and A.C. Ouwehand, *Streptococcus mutans, caries and simulation models.* Nutrients, 2010. **2**(3): p. 290-298.
29. Åberg, C.H., P. Kelk, and A. Johansson, *Aggregatibacter actinomycetemcomitans: virulence of its leukotoxin and association with aggressive periodontitis.* Virulence, 2014. **6**(3): p. 188-195.
30. *National Institutes of Health Consensus Development Conference statement. Diagnosis and management of dental caries throughout life, March 26-28, 2001.* J Am Dent Assoc, 2001. **132**(8): p. 1153-61.
31. Woelfel, J.B. and R.C. Scheid, *Dental anatomy its relevance to dentistry*. 2007, Philadelphia: Wolters Kluwer : Lippincott Williams & Wilkins.
32. Shah, N., N. Bansal, and A. Logani, *Recent advances in imaging technologies in dentistry.* World journal of radiology, 2014. **6**(10): p. 794-807.
33. Kielbassa, A.M., et al., *External and internal resin infiltration of natural proximal subsurface caries lesions: A valuable enhancement of the internal tunnel restoration.* Quintessence Int, 2017. **48**(5): p. 357-368.
34. Knosel, M., A. Eckstein, and H.J. Helms, *Durability of esthetic improvement following Icon resin infiltration of multibracket-induced white spot lesions compared with no therapy over 6 months: a single-center, split-mouth, randomized clinical trial.* Am J Orthod Dentofacial Orthop, 2013. **144**(1): p. 86-96.
35. Paris, S. and H. Meyer-Lueckel, *Masking of labial enamel white spot lesions by resin infiltration--a clinical report.* Quintessence Int, 2009. **40**(9): p. 713-8.
36. Shivanna, V. and B. Shivakumar, *Novel treatment of white spot lesions: A report of two cases.* J Conserv Dent, 2011. **14**(4): p. 423-6.
37. Cazzolla, A.P., et al., *Efficacy of 4-year treatment of icon infiltration resin on postorthodontic white spot lesions.* BMJ Case Rep, 2018. **2018**.
38. Kielbassa, A.M., J. Müller, and C.R. Gernhardt, *Closing the gap between oral hygiene and minimally invasive dentistry: A review on the resin infiltration technique of incipient (proximal) enamel lesions.* Quintessence Int, 2009. **40**(8): p. 663-681.
39. Fan, Y., *Effects of Different Finishing Procedures and Materials on Surface Roughness of Infiltrated Subsurface Bovine Enamel Lesions* 2010, Charité - Universitätsmedizin Berlin.
40. B Gray, G. and R. Shellis, *Infiltration of resin into white spot caries-like lesions of enamel: An in vitro study*. Vol. 10. 2002. 27-32.

41. Meyer-Lueckel, H. and S. Paris, *Improved Resin Infiltration of Natural Caries Lesions.* Journal of Dental Research, 2008. **87**(12): p. 1112-1116.
42. DMG America: Icon Information Patient Site. *Downloads, Product Brochure [Internet]*. [cited 2019 May 20]; Available from: http://drilling-no-thanks.info/doctors/Downloads_doctors.php.
43. Sigma Aldrich. *Triethylene glycol dimethacrylate [Internet]*. [cited 2019 12 May]; Available from: https://www.sigmaaldrich.com/catalog/product/sigma/t5537?lang=en&region=CA.
44. Sigma Aldrich. *Camphorquinone [Internet]*. [cited 2019 12 May]; Available from: https://www.sigmaaldrich.com/catalog/product/aldrich/124893?lang=en&region=CA.
45. Sigma-Aldrich. *trans-2-[3-(4-tert-Butylphenyl)-2-methyl-2-propenylidene]malononitrile [Internet]*. [cited 2019 May 28]; Available from: https://www.sigmaaldrich.com/catalog/product/sial/87884?lang=en&region=CA.
46. Sigma-Aldrich. *2,5-Dihydroxybenzoic acid [Internet]*. [cited 2019 May 28]; Available from: https://www.sigmaaldrich.com/catalog/product/aldrich/149357?lang=en&region=CA.
47. Sigma-Aldrich. *Dithranol [Internet]*. [cited 2019 May 28]; Available from: https://www.sigmaaldrich.com/catalog/product/aldrich/259209?lang=en&region=CA.
48. Sigma-Aldrich. *2',4',6'-Trihydroxyacetophenone monohydrate [Internet]*. [cited 2019 May 28]; Available from: https://www.sigmaaldrich.com/catalog/product/sial/91928?lang=en&region=CA.
49. ProteoChem - Crosslinking Protein Biology and Chemistry. *CHCA Matrix Product Information Sheet & General Protocol [Internet]*. [cited 2019 27 May]; Available from: http://www.proteochem.com/chca5x10mg-p-170.html.
50. Material Safety Data Sheet - DMG Dental. *Icon Dry - Material Safety Data Sheet [Internet]*. [cited 2019 Mar 22]; Available from: https://uk.dmg-dental.com/en-gb/downloads/material-safety-data-sheet/.
51. DMG America: Icon Information Patient Site. *Downloads, Instructions for Use [Internet]*. [cited 2019 May 20]; Available from: http://drilling-no-thanks.info/doctors/Downloads_doctors.php.
52. Okamoto, K. *MALDI Mass Spectrometry of Synthetic Polymers*.

53. Payne, M.E. and S.M. Grayson, *Characterization of Synthetic Polymers via Matrix Assisted Laser Desorption Ionization Time of Flight (MALDI-TOF) Mass Spectrometry.* Journal of visualized experiments : JoVE, 2018(136): p. 57174.

54. Dey, M., J.A. Castoro, and C.L. Wilkins, *Determination of Molecular Weight Distributions of Polymers by MALDI-FTMS.* Analytical Chemistry, 1995. **67**(9): p. 1575-1579.

55. https://chemistry.mit.edu/. *MALDI -TOF SAMPLE PREPERATION GUIDE, General prep for non-water soluble organic and aromatic polymer samples*. [cited 2019 May 20]; Available from: https://chemistry.mit.edu/wp-content/uploads/2018/08/DCIF-MALDI_sample_prep_0.pdf.

56. Home. Dental Milestones Guaranteed. *Downloads, Safety datasheets [Internet]*. [cited 2019 May 20]; Available from: https://www.dmg-dental.com/fileadmin/user_upload/shared/MSDS/en/MSDS_CPF_IconInfiltrant_2600_EN.pdf.

57. Rivas, D., et al., *Using a polymer probe characterized by MALDI-TOF/MS to assess river ecosystem functioning: From polymer selection to field tests.* Science of The Total Environment, 2016. **573**: p. 532-540.

58. Julien De Winter, G.D., Florian Boon, Olivier Coulembier, Philippe Dubois, Pascal Gerbaux; , *MALDI-ToF analysis of polythiophene: use of trans-2-[3-(4-t-butyl-phenyl)-2-methyl- 2-propenylidene]malononitrile—DCTB—as matrix.* JOURNAL OF MASS SPECTROMETRY, 2011. **46**(3): p. 237-246.

59. Brandt, H., T. Ehmann, and M. Otto, *Investigating the effect of mixing ratio on molar mass distributions of synthetic polymers determined by MALDI-TOF mass spectrometry using design of experiments.* Journal of the American Society for Mass Spectrometry, 2010. **21**(11): p. 1870-1875.

60. Department of Chemistry Home Page - Department of Chemistry. *MALDI –TOF SAMPLE PREPARATION GUIDE, Matrix preparation, trans-2-[3-(4-tert-Butylphenyl)-2-methyl-2-propenylidene]malononitrile- DCTB* [cited 2019 May 20]; Available from: http://www.chem.ox.ac.uk/spectroscopy/mass-spec/Services_allFiles/Protocols/MALDI%20spot%20sample%20micro%20MALDI%20Waters.pdf.

61. Biomedical Mass Spectrometry Resource | WUSTL.edu. *MALDI Sample Preparation Dried-Droplet Crystallization [Internet]*. [cited 2019 May 18]; Available from: https://msr.dom.wustl.edu/maldi-sample-preparation-dried-droplet-crystallization/.

62. Hankin, J.A., R.M. Barkley, and R.C. Murphy, *Sublimation as a method of matrix application for mass spectrometric imaging*. Journal of the American Society for Mass Spectrometry, 2007. **18**(9): p. 1646-1652.

63. Lu, K., *OPTIMIZATION OF SUBLIMATION CONDITIONS FOR SURFACE LAYER MATRIX-ASSISTED LASER DESORPTION IONIZATION TIME OF FLIGHT MASS SPECTROMETRY IMAGING (SL-MALDI-TOF MSI) OF POLYMER SURFACES*. 2018.